Optimizing offshore wind farm transportation and installation strategies including manufacturing ports

Using a rolling horizon simulation model

Tenzin Frijlink

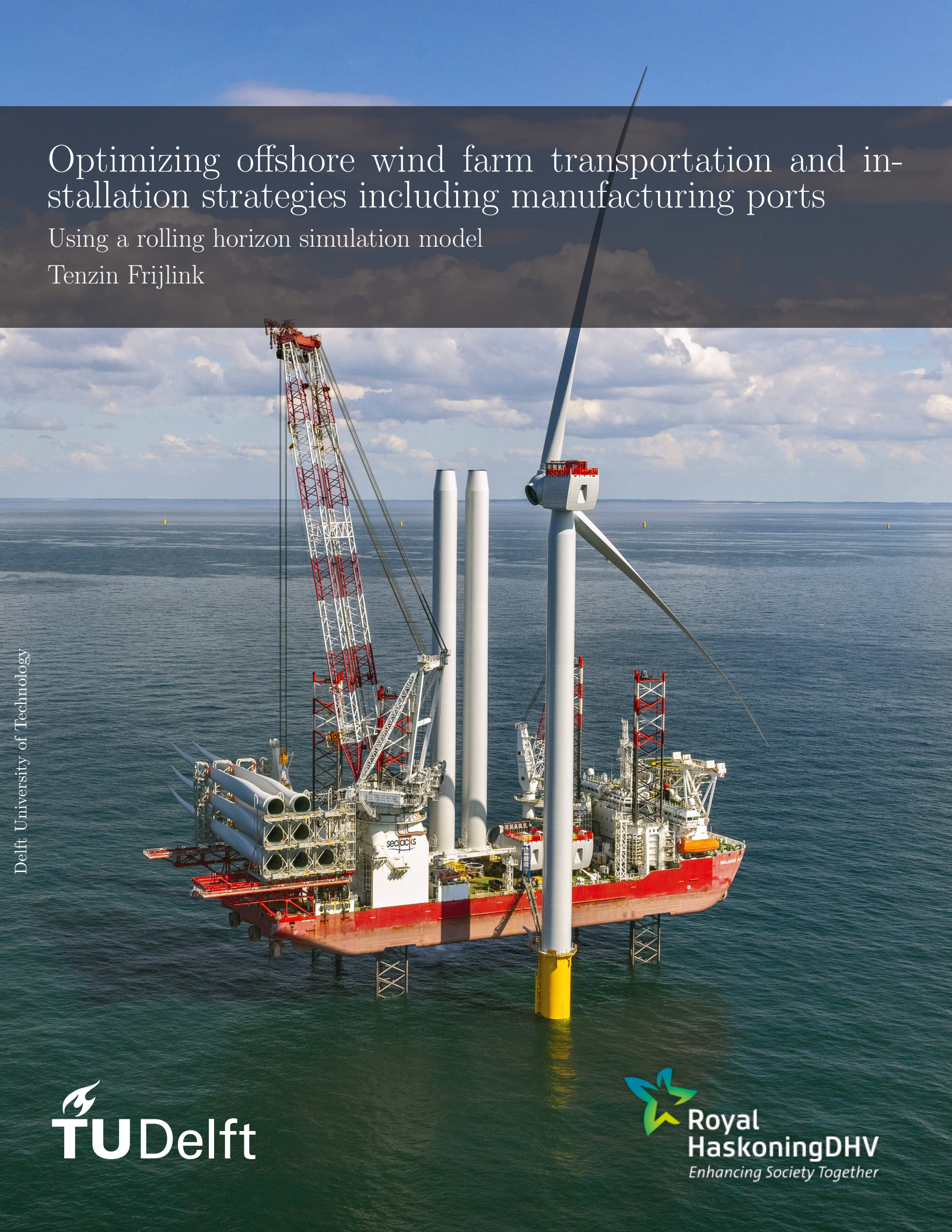

Delft University of Technology

TU Delft

Royal HaskoningDHV
Enhancing Society Together

Optimizing offshore wind farm transportation and installation strategies including manufacturing ports

Delft University of Technology

Master's Thesis

Transport, Infrastructure and Logistics
Specialisation Logistic Systems

Author	
Tenzin Frijlink	4718976
Supervisors	
Lóri Tavasszy	TU Delft
Stefano Fazi	TU Delft
Mark Duinkerken	TU Delft
Leon Lammers	Royal HaskoningDHV

Abstract

The installation rate of offshore wind energy has to be quadrupled by 2030 to meet the green climate ambitions of European countries, but this growth is hindered by logistical challenges. Therefore, this study explores how two transportation and installation strategies, shuttling and feedering, affect the installation rate with the inclusion of manufacturing ports. Shuttling is where the installation vessel collects components itself at a port, and feedering is where the installation vessel remains offshore and gets supplied directly via feeder vessels. This is a novel approach as feedering and manufacturing ports are often not considered and production rates at manufacturing ports have not been considered at all. A rolling horizon simulation model is developed, which uses a Markov simulation model for weather forecasting, with a 72.92% forecast accuracy over two weeks, and a greedy algorithm for transportation and installation optimization. Results indicate that accurate initial buffer calculations, depending on the production rate at the manufacturing ports and project-dependent characteristics, can increase the installation rate significantly for either strategy. Shuttling becomes more efficient than feedering if the distance between the manufacturing ports and the offshore wind farm is too large or the size of the feeder vessels is too small. Feedering is more efficient in all other circumstances and, on average, results in a 9.2% higher installation rate and reduces project duration by 29 days compared to shuttling.

May 16, 2024

Cover: Installation vessel Scylla installing a wind turbine at Hollands Kust Noord (Eneco, 2023)

TU Delft

Executive Summary

European countries surrounding the North Seas have set a goal of installing at least 120 gigawatts (GW) of offshore wind energy by 2030 (NSEC, 2023). However, only 30GW is installed, which means a fourfold scale-up is required in the upcoming coming years. However, this scale-up is faced with many industry challenges (CEIF, 2022). The challenges addressed in this report are (i) a limited fleet of Wind Turbine Installation Vessels (WTIVs), (ii) bottlenecks in port capacity and (iii) weather dependency of operations. The challenges are listed below in more detail:

1. **There is a limited fleet of wind turbine installation vessels**
   Currently, the Wind Turbine Installation Vessel (WTIV) fleet consists of 21 vessels, with over half incapable of installing turbines larger than 15MW, as indicated by a market study from H-Blix (2022). Despite the construction of seven new WTIVs in the coming years, all capable of installing 15MW+ turbines, a gap of roughly four WTIVs remains, resulting in an unmet installation capacity of 6.4GW of offshore wind energy yearly.

2. **Ports will be a significant bottleneck in the future**
   A recent port capacity study by Royal HaskoningDHV for NSEC has emphasized that ports will become a serious bottleneck for offshore wind development (NSEC, 2023). Currently, 600 hectares of storage area are available, with 200 hectares being added in the coming years. However, between 850 and 1300 hectares of storage area is needed, which results in a storage area deficit of at least 50 and up to 500 hectares.

3. **The construction of wind turbines is heavily dependent on weather conditions**
   Weather-related delays account for over 20% of the time required for offshore wind projects (Lerche et al., 2022). This is not surprising as wind turbines are installed where strong winds occur, but this also makes installation more difficult as operational limits apply. WTIVs can have day rates of over €250,000, so are a a large expenditure. Especially if vessels have to be rented longer than expected, due to bad weather conditions. Weather forecasts are only 50% accurate after 10 days (Ritchie, 2024), so it is difficult to prevent weather-related delays.

Transportation and installation strategies: shuttling and feedering

In the future, these challenges could be addressed by expanding the installation vessel fleet, creating more port capacity and having more accurate weather forecasts. However, in the short term, the transportation and installation strategy used is much more relevant. Two transportation and installation strategies for offshore wind projects are explored: shuttling and feedering. Each comes with its own set of (dis)advantages. Figure I illustrates the difference in logistics between these two strategies. Rectangles indicate physical locations, whereas rounded rectangles indicate which vessels are required for transportation or transshipment.

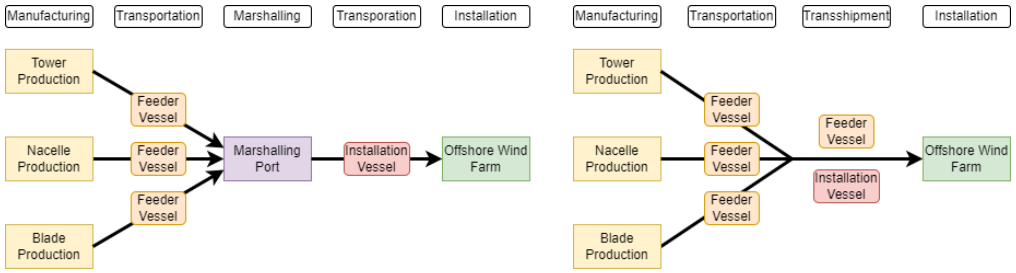

Figure I: Shuttling and feedering logistics respectively

With shuttling, manufacturing ports supply the marshalling port via feeder vessels (FVs). This approach involves the WTIV shuttling, hence the name, between the marshalling port and the offshore wind farm. Increased distances between the marshalling port and offshore wind farm (OWF) pose challenges for shuttling as the WTIV spends relatively more time sailing than installing, which does not utilize the WTIV effectively as it is meant for installation. Furthermore, the utilization of the WTIV is closely tied to the inventory management at the marshalling port.

With feedering, the manufacturing ports directly supply the WTIV, which remains offshore, via the FVs. A key advantage of this strategy is that no marshalling port is required. However, now there are two weather-dependent operations, namely transshipment and installation, potentially reducing the time spent installing, since good weather conditions are now used for transshipment instead of installation. Additionally, this means all inventory has to be stored at the manufacturing ports, which often have limited available space.

Key findings

Therefore, this report explores how manufacturing ports, shuttling and feedering affect the installation rate. This provides specific insights to address each challenge:

1. **Limited fleet of wind turbine installation vessels**

   Due to the limited WTIV fleet, the installation rate has to be increased significantly to meet the 2030 climate ambitions. By only starting the installation process with a certain buffer already available, the installation rate increases significantly for both shuttling and feedering, as now components are readily available for installation.

   Feedering generally increases the installation rate and reduces project duration by 9.21% compared to shuttling. This shortens project duration by 29 days on average, which could save millions. Additionally, feedering is less dependent on the quality of the weather forecast and weather conditions in general, so is also more robust than shuttling.

   Shuttling starts being more efficient than feedering if the manufacturing ports are located more than 1000 km from the OWF and the marshalling port lies within 500 km of the OWF. However, if manufacturing ports lie within roughly 500 km of the OWF, feedering is more

effective. Additionally, if the size of the feeder vessels is too small, shuttling also becomes more efficient than feedering.

2. **Limited port capacity**
   Results show that production rates have a significant impact on the required port capacity. If the production rate is 54 of 81 hours, a limited amount of port capacity is needed as just-in-time logistics can be used. However, if the production time is 162 hours per component, buffers of up to 70% of the project size could be required. This translates to roughly 20ha of storage area for a 1GW project, which might not be available in the future.

   Results also show that the required port capacity is directly related to the production time and initial buffer. Thus calculating the required initial buffer accurately will also result in the lowest amount of reserved port capacity, whilst optimizing the installation rate.

   Since shuttling generally has a lower installation rate than feedering, it also requires less initial buffer. So if port capacity is an issue, shuttling should be considered, but this does result in a longer project duration. So whilst it might help for port capacity, it could increase the pressure on the WTIV fleet.

3. **Dependence on weather conditions**
   Weather conditions play a significant role in the installation rate and project duration of offshore wind projects. Feedering in general performs better than shuttling in any simulated year. Compared to an average year, the installation rate increases by 3.1 and 11.7% for shuttling and feedering respectively in a good year. In a bad year, installation rates decrease by 13.5 and 6.5% respectively. This means that feedering benefits more from good weather and is affected less by worse weather.

   Moreover, increasing the accuracy of the weather forecast can increase the installation rate by 5.05% on average. Additionally, shuttling benefits much more from higher-quality forecasts, as this likely allows for a better choice of when to sail out for installation.

Conclusion

The installation rate of offshore wind turbines has to be quadrupled in the coming years. However, if the production rate is insufficient, large port capacities are required, so increasing the production rate could address the port capacity bottleneck. Additionally, shuttling is more efficient than feedering if the manufacturing ports are located more than 1000 km from the offshore wind farm and the marshalling port lies within 500 km of the offshore wind farm or if the feeder vessels are small. In all other circumstances, feedering outperforms shuttling and is less weather-dependent. Feedering, on average, results in a 9.2% higher installation rate and reduces project duration by 29 days. Therefore, feedering should be considered as a feasible transportation and installation strategy to increase the installation rate.

Contents

1 Introduction

European countries surrounding the North Seas have set a goal of installing at least 120 gigawatts (GW) of offshore wind energy by 2030 (NSEC, 2023). However, only 30GW is installed, which means a fourfold scale-up is required in the upcoming years, as illustrated in Figure 1a. However, this scale-up is faced with many industry challenges (CEIF, 2022). The challenges addressed in this report are (i) a limited fleet of Wind Turbine Installation Vessels (WTIVs), (ii) bottlenecks in port capacity and (iii) weather-dependency of operations. To overcome these challenges, insights into the wind turbine installation process are essential. Wind turbine installation refers to the installation of tower, nacelle and three blades by the WTIV, as shown in Figure 1b.

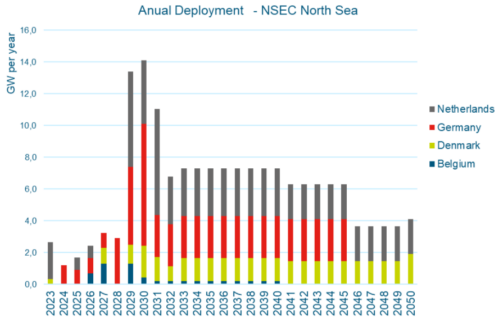

(a) Annual wind energy deployment for the NSEC countries (NSEC, 2023)

(b) The third, and last, blade of a wind turbine is being installed (Van Oord, 2020)

Figure 1: Required NSEC installation rates (1a) and wind turbine installation by a WTIV (1b)

This report explores shuttling, where the WTIV collects components itself at a port, and feedering, where the WTIV remains offshore and gets supplied directly via feeder vessels. The risk of shuttling is that the WTIV spends more time sailing than installing, whereas for feedering the risk is that there are insufficient weather conditions to both transship and install offshore. Additionally, the location of and production rate of components at the manufacturing ports are of great importance to installation efficiency (Hrouga & Bostel, 2021). Therefore, this report explores how manufacturing ports, shuttling and feedering affect the installation rate.

To do so, this report uses a rolling horizon simulation model, which uses a Markov simulation model for weather forecasting and a greedy algorithm for transportation and installation optimization. Key factors for each strategy, such as port locations, buffer size and vessel size are identified. Results show that feedering is generally more efficient than shuttling and can reduce project duration by weeks, potentially saving millions, but project-dependent nuances apply.

First, Section 2 elaborates on the contextual background and research methodology of this report. Second, Section 3 reviews the state-of-the-art literature. Third, in Section 4, the mathematical model is defined. Fourth, Section 5 describes the relevant case studies. Fifth, Section 6 describes the rolling horizon simulation method. Sixth, the results and set-up of the computational experiments are elaborated on in Section 7. Seventh and last, the key findings are discussed in Section 8.

2 Contextual background and research methodology

In this section, the problem and research goals are identified. Firstly, Section 2.1 elaborates on the cause of the industry challenges. Secondly, the research scope is defined in Section 2.2. Thirdly, Section 2.3 delves further into the two transportation and installation strategies. Fourthly, Section 2.4 describes the operational steps of the wind turbine installation process. Fifthly, Section 2.5 identifies the relevant research gaps and places this report within the existing literature. Sixthly and lastly, the main research question and supporting research questions are formulated in Section 2.6.

2.1 Challenges in offshore wind energy expansion

The cause of the three challenges addressed in this report, (i) a limited fleet of WTIVs, (ii) bottlenecks in port capacity and (iii) weather-dependency of operations, is discussed below.

1. **There is a limited fleet of wind turbine installation vessels**
   Currently, the Wind Turbine Installation Vessel (WTIV) fleet consists of 21 vessels, with over half incapable of installing turbines larger than 15MW, as indicated by a market study from H-Blix (2022). Despite the construction of seven new WTIVs in the coming years, all capable of installing 15MW+ turbines, a gap of roughly four WTIVs remains, resulting in an unmet installation capacity of 6.4GW of offshore wind energy yearly.

2. **Ports will be a significant bottleneck in the future**
   A recent port capacity study by Royal HaskoningDHV for NSEC has emphasized that ports will become a serious bottleneck for offshore wind development (NSEC, 2023). Currently, 600 hectares of storage area are available, with 200 hectares being added in the coming years. However, between 850 and 1300 hectares of storage area is needed, which results in a storage area deficit of at least 50 and up to 500 hectares.

3. **The construction of wind turbines is heavily dependent on weather conditions**
   Weather-related delays account for over 20% of the time required for offshore wind projects (Lerche et al., 2022). This is not surprising as wind turbines are installed where strong winds occur, but this also makes installation more difficult as operational limits apply. WTIVs can have day rates of over €250,000, so are a a large expenditure. Especially if vessels have to be rented longer than expected, due to bad weather conditions. Weather forecasts are only 50% accurate after 10 days (Ritchie, 2024), so it is difficult to prevent weather-related delays.

In the future, these challenges could be addressed by expanding the installation vessel fleet, creating more port capacity and having more accurate weather forecasts. However, in the short term, challenge-specific solutions and insights are needed to meet the ambitious green climate ambitions. The connecting factor is the utilization of the WTIV as this affects for which period the vessel is required, what port capacity is required and how weather conditions affect the transportation and installation process. As such, the utilisation of the WTIV is the main focus of this report.

2.2 Research scope: manufacturing, transportation and installation of turbines

In this section, the life cycle stages of offshore wind farms are described. Additionally, the transportation and installation stages are highlighted, as well as the underlying wind turbine installation stages, which are the focus of this report and highlighted in yellow, as illustrated in Figure 2

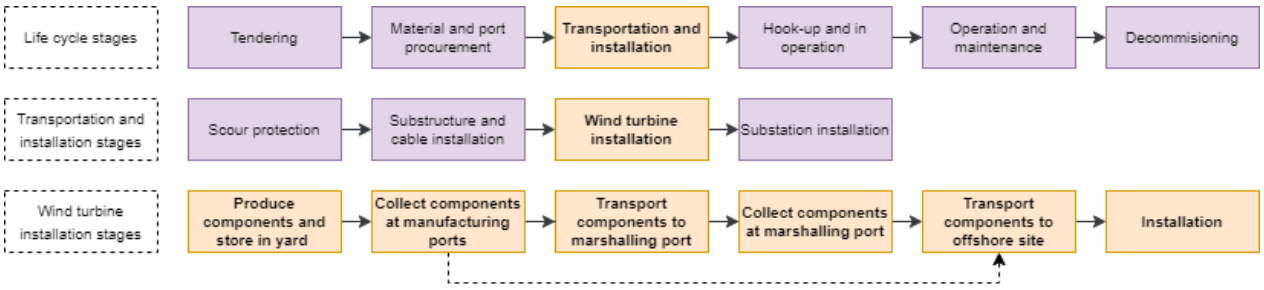

Figure 2: Stages of offshore wind farm projects from the life cycle down to wind turbine installation. The research scope is highlighted in yellow. The white dotted box shows which stages are highlighted. Based on Figure 2 from Tjaberings et al. (2022). The dotted line indicates that it is possible to directly transport components from manufacturing ports to the offshore site.

Initially, a developer, often an energy company, acquires a tender that specifies a geographical plot for the construction of a certain amount of MW. Then, the developer needs to procure the required materials and port capacity. This task is commonly delegated to several specialized sub-contractors, each working independently. For example, Vestas can be asked to manufacture the turbines, and Seaway to manufacture foundations. Once all components are transported and installed, the wind turbines need to be connected to the power grid and put into operation. Regular maintenance checks and repairs are performed during the operation of the wind farm. At the end of their life cycle, the wind turbines are decommissioned. This report looks at the transportation and installation stage as this makes up 20% of the total costs (Sarker & Faiz, 2017).

For the transportation and installation, first scour protection is applied, and then the substructure, including the transition pieces, and cables are installed. Afterwards, the wind turbines are installed on top of the foundations. Last, the substation is installed, which collects the cables from all wind turbines and serves as the connection to the shore. Wind turbine installation is the most complex transportation and installation stage (Rippel, Jathe, L'tjen, & Freitag, 2019), as it requires sequential weather-dependent installation operations and is, therefore, the focus of this report.

Wind turbine installation consists of several stages. Initially, components are collected at manufacturing ports and then transported to the marshalling port. Then, at the marshalling port, the components are collected and transported by the installation vessel to the offshore site, so-called shuttling. Alternatively, components can be transported directly from manufacturing ports to the installation vessel at the offshore site, a process referred to as feedering. Finally, the wind turbines are installed, which is dependent on weather conditions as operational limitations apply.

2.3 Transportation and installation strategies: shuttling and feedering

Two transportation and installation strategies for offshore wind projects are explored: shuttling and feedering. Each comes with its own set of (dis)advantages. Figure 3 illustrates the difference in logistics between these two strategies. Rectangles indicate physical locations, whereas rounded rectangles indicate which vessels are required for transportation or transshipment.

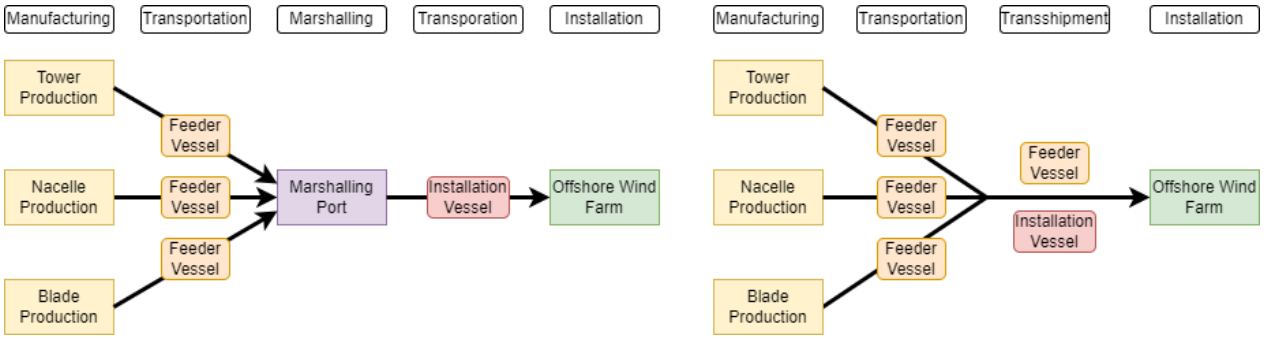

Figure 3: Shuttling and feedering logistics respectively

With shuttling, manufacturing ports supply the marshalling port via feeder vessels (FVs). This approach involves the WTIV shuttling, hence the name, between the marshalling port and the offshore wind farm. Increased distances between the marshalling port and offshore wind farm (OWF) pose challenges for shuttling as the WTIV spends relatively more time sailing than installing, which does not utilize the WTIV effectively as it is meant for installation. Furthermore, the utilization of the WTIV is closely tied to the inventory management at the marshalling port. If insufficient inventory is available, no installation is possible.

With feedering, the manufacturing ports directly supply the WTIV, which remains offshore, via the FVs. A key advantage of this strategy is that no marshalling port is required. However, now there are two weather-dependent operations, namely transshipment and installation, potentially reducing the time spent installing, since good weather conditions are now used for transshipment instead of installation. Additionally, this means all inventory has to be stored at the manufacturing ports, which often have limited available space. So whilst feedering in Figure 3 might look simple, it has more weather-dependent operations than shuttling.

In practice, shuttling is the commonly used strategy, as it allows for significant buffers of components in the marshalling port, which ensures components are always available, and a decoupling between the WTIV and FVs. This makes it easier to have a contract with a manufacturer, as now fixed times to collect components can be determined. This is much more difficult for feedering, as it is not known in advance when the FVs will return from supplying the WTIV, due to the weather-dependent transshipment. This is a major point of concern for experts in the field, as weather conditions for offshore transshipment are even more constraining than for regular installation. This could result in good-weather windows being used for transshipment instead of installation, not utilizing the WTIV effectively.

2.4 Operational steps

The wind turbine installation process comprises three essential sequential stages: manufacturing, transportation, either via shuttling or feedering, and installation. The operational steps per stage are illustrated in Figure 4, with colours indicating the responsible vessel or port for each operation. Recall that three components are required for wind turbine installation: tower, nacelle and blades, which also need to be installed in this order (Rippel, Jathe, L'tjen, & Freitag, 2019).

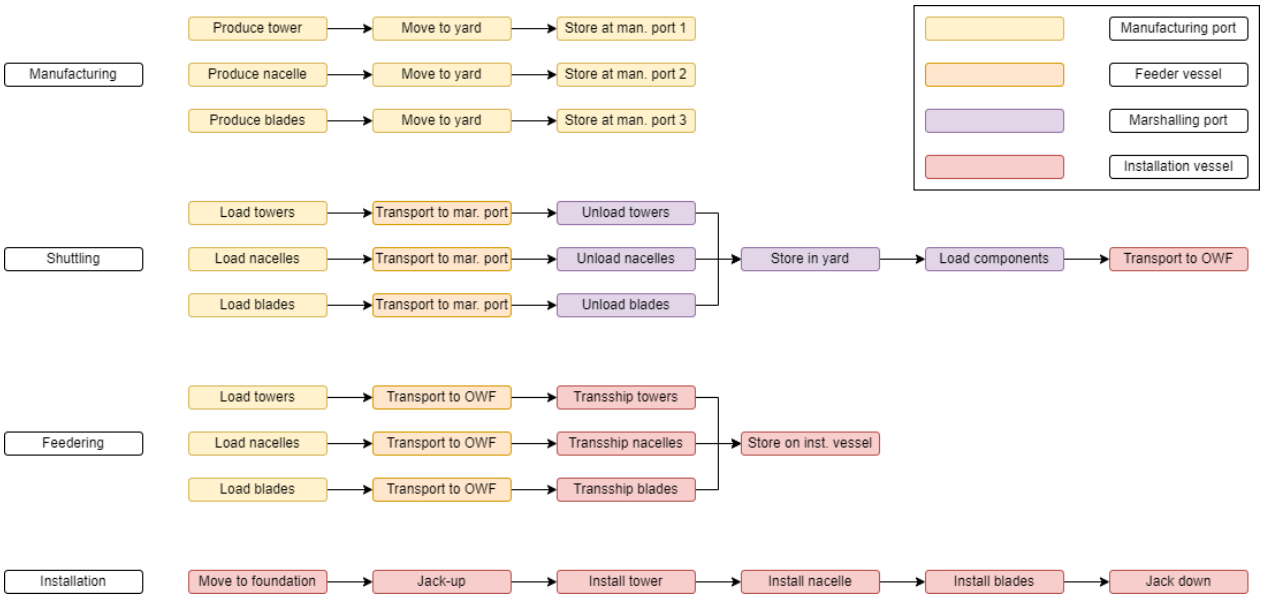

Figure 4: Illustration of operational steps per stage, the colours indicate which vessel or port is used. The legend shows what each colour represents

Notably, the manufacturing and installation are independent of the method of transportation. The steps required for manufacturing are to produce a component, move it to the storage yard and then store it in the respective manufacturing port until the component gets collected. For installation, the WTIV first has to move to the available foundation, then jack-up, install the tower, nacelle, and blades and finally jack down. For both installation and installation, it is not relevant how the components get transported, which is why they are independent.

The key distinction in operational steps lies in the transportation strategies. Shuttling involves the use of a marshalling port, resulting in additional intermediate steps. I.e. components get transported from the manufacturing ports to the marshalling port, then stored, until the WTIV is ready to collect them. Whilst feedering transports the components directly from the manufacturing ports to the WTIV, eliminating the need for a marshalling port, leading to fewer intermediate steps.

Note that for feedering the feeder vessels travel between the manufacturing ports and OWF, whilst for shuttling these vessels travel between the manufacturing ports and marshalling port. So even though feedering has fewer steps, operations are more complex to schedule since both the feeder vessel and WTIV have to be available at the same time for transshipment.

2.5 Research gap

To address the identified challenges in offshore wind energy expansion, it is imperative to delve deeper into the existing literature. The results of this analysis are synthesized in Table 1, which provides a thorough overview of the existing literature, the specific methodologies are discussed in Section 3.2. Firstly, it is indicated whether a simulation-based or mathematical-based optimization is used. Secondly, it is indicated which of the following aspects are included in the research: weather conditions, manufacturing ports, shuttling, feedering and port capacity.

Table 1: Overview of T&I literature from 2017 onwards

Author	Sim	Math	Weather	Shuttling	Feeder	Manu	Port cap.
Beinke et al. (2017)	✓		✓	✓		✓	
Irawan et al. (2017)		✓	✓	✓			
Quandt et al. (2017)	✓		✓	✓		✓	✓
Ursavas (2017)		✓	✓	✓			
Barlow et al. (2018)	✓	✓	✓	✓			
Oelker et al. (2018)	✓		✓	✓	✓	✓	
Rippel, Jathe, L'tjen, & Freitag (2019)	✓	✓	✓	✓			
Oelker et al. (2020)	✓		✓	✓			✓
Tjaberings et al. (2022)	✓		✓	✓	✓		
This report	✓	✓	✓	✓	✓	✓	✓

Note. The first column shows the author, and the second and third columns indicate whether the study is simulation or mathematical optimization-based. The last columns indicate if weather conditions, manufacturing ports, shuttling, feedering and port capacity were considered respectively.

Based on Table 1, it might seem trivial to include weather conditions. However, there is a large diversity in how these are taken into account. For instance, Beinke et al. (2017), Oelker et al. (2018), Oelker et al. (2020) and Tjaberings et al. (2022) simply use historical data as the forecast data. This is not realistic as forecasts are only 50% accurate for a 10-day planning horizon (Ritchie, 2024). Ursavas (2017) randomly generates weather conditions, for Quandt et al. (2017) it is unclear how the weather forecasts are made, Irawan et al. (2017) randomly generate the forecasts based on historical probabilities. Only Barlow et al. (2018) and Rippel, Jathe, L'tjen, & Freitag (2019) have a weather forecasting method specified, which is much more realistic as it includes the uncertainty.

It can also be observed that all papers take into account shuttling, but here some variation also applies. Beinke et al. (2017), Irawan et al. (2017), Quandt et al. (2017), Ursavas (2017), Oelker et al. (2018), Oelker et al. (2020) and Tjaberings et al. (2022) all use the basic shuttling principle. I.e., the installation vessel comes to port, loads to its maximum capacity, goes offshore to install and returns once empty. Barlow et al. (2018) uses a different approach where vessels are first assigned to a task and the planning is made afterwards. Rippel, Jathe, L'tjen, & Freitag (2019) use a flexible

planning based on the forecast weather conditions. In both of these approaches the installation vessel is not necessarily fully loaded and can potentially make better use of the forecast weather conditions and the planning can capture this uncertainty.

Feedering is only considered by Oelker et al. (2018) and Tjaberings et al. (2022). Tjaberings et al. (2022) performs an in-depth simulation of substructure transportation strategies, but only consider a singular port for this purpose. As such, feedering happens between the marshalling port and the installation vessel. This neglects that feedering could potentially result in not requiring such a port, as components can be collected directly from the manufacturing ports, which results in different logistics. This approach is adopted by Oelker et al. (2018), who find that with a sufficiently large feeder vessel fleet, feedering is up to 20% more efficient than shuttling.

Only Beinke et al. (2017), Quandt et al. (2017) and Oelker et al. (2018) take manufacturing ports into account to some extent. All of these papers acknowledge there are multiple components and that these have to be collected at different locations. However, all papers also consider components to always be available in the manufacturing ports, so do not consider production times and potential implications of this, thus implicitly assuming components are always available. This is not realistic as CEIF (2022) indicate the manufacturing rate will be a significant bottleneck in the future.

Quandt et al. (2017) and Oelker et al. (2020) are the only papers taking port capacity into account explicitly. Rippel, Jathe, L'tjen, & Freitag (2019) do consider berth availability, but this is outside the scope of this report. Quandt et al. (2017) find that proper inventory management at the manufacturing port could lead to 20% less required port capacity. Oelker et al. (2020) find that due to the increasing size of turbines and project size, the concept of classic marshalling ports might not be feasible in the future due to limited port capacity, which is in line with NSEC (2023).

There are three main takeaways from the reviewed literature. Firstly, most papers only allow one transportation strategy to be selected and therefore use shuttling. Secondly, most papers do not consider manufacturing ports and even papers that do, assume production times are sufficiently fast to always have components available. Thirdly, port capacity is often not taken into account, whilst this is a significant bottleneck and could limit project duration. Building upon the challenges outlined in Section 2.1, it becomes apparent that the identified gaps in existing literature align closely with the ongoing challenges in offshore wind energy expansion. Addressing these challenges using the novel approach of this report could provide valuable insights concerning the wind turbine transportation and installation process since it uses a holistic view of the supply chain.

2.6 Research goal and questions

The challenges in increasing the installation rate align closely with the gaps in existing literature. The installation rate is defined as the number of wind turbines installed per time unit. Manufacturing ports, shuttling and feedering, have come up as important aspects to consider to increase the installation rate and fill these gaps. Therefore, the main research question of this report is: **How do manufacturing ports, shuttling and feedering impact the installation rate?**

The main research question is answered in Section 8, based on the insights of Supporting Research Questions (S-RQs). These questions help analyze relevant literature, map operational steps, transform these into a suitable method, and evaluate results to address the motivating challenges behind this report. Below the S-RQs are listed in detail along with their methodology.

S-RQ1 **Which methods are currently used to optimize offshore wind farm logistics or related problems and what are their respective strengths?**
This question delves into the existing literature and aims to identify the models and methodologies that have been employed in optimizing offshore wind farm logistics and what their (dis)advantages are. This question is answered via a literature review in Section 3.

S-RQ2 **How can the operational steps be translated to a realistic mathematical model?**
This question specifically aims to comprehend the operational steps essential for installing offshore wind turbines and translating these steps into a realistic mathematical model. The operational steps are defined through a mix of literature and non-formal expert interviews, after which the mathematical model is defined, verified and validated in Section 4.

S-RQ3 **Which realistic and relevant case studies can be identified for analysis?**
This question aims to construct test instances, such that the model can be applied to real-life tests for validation purposes. Moreover, it ensures that the final results are reliable, as the case studies have been set up for different locations, vessels and turbine sizes. These instances, along with their motivation and characteristics are described in Section 5.

S-RQ4 **Which method is suitable to optimize transportation and installation logistics for an offshore wind farm?**
This question builds upon the knowledge gathered in the previous questions and seeks to identify the most suitable model characteristics for addressing the specific requirements of this report. This question is answered by analyzing the critical evaluation of existing models, based on the review of relevant literature from Section 3.4, to come to the most suitable method for this report. The methodology, verification and validation are discussed in Section 6.

S-RQ5 **What insights can be derived regarding the challenges in offshore wind expansion?**
This final question ties together the information obtained from the operational steps and the implemented model. It aims to extract meaningful recommendations and insights that address the challenges highlighted in offshore wind expansion, which is both relevant for practical applications as well as for future research. To do so, real-life test instances are set up to gain meaningful insights in combination with numerous experiments. The test instances, experimental set-up, computation results and insights are provided in Section 7.

3 Related work

In this section methods used to solve the wind turbine installation problem and related problems are reviewed to answer S-RQ1. First, research on marshalling and manufacturing ports is discussed in Section 3.1. Second, works on transportation and installation strategies are discussed in Section 3.2. Third, approaches from related problems are discussed in Section 3.3. Fourth and last, suitable papers, and their models, for this report are discussed and synthesized in Section 3.4.

3.1 Manufacturing and marshalling ports

Ports play a key role in reliable supply-chain management operations (Drunsic et al., 2016). Hrouga & Bostel (2021), after a literature review, emphasize the importance of considering more aspects of the supply chain, such as manufacturing ports. Additionally, there are significant lead times for materials in manufacturing ports (CEIF, 2022), which is important to consider.

Jiang (2021) analyse the full installation process of offshore wind farms and find that, due to the increase in the size of wind turbines, marshalling ports are critical in the future. This is a similar conclusion to Oelker et al. (2020) and NSEC (2023), which both state marshalling port capacity could be insufficient in the future. Beinke et al. (2020) use a supply chain-oriented approach and found that information sharing on weather conditions, storage capacity and vessel availability has a large influence on port utilisation. Therefore, it is important to consider both manufacturing and marshalling ports to accurately model the supply chain of offshore wind farms.

3.2 Transportation and installation

Limited research has been performed on the general logistics of offshore wind farms (Vis & Ursavas, 2016). Moreover, there are even fewer papers focusing on transportation and installation, which makes up almost 20% of the total costs (Sarker & Faiz, 2017). The transportation and installation planning of offshore wind farms requires unique meteorological and oceanographic conditions compared to other planning problems (Beinke et al., 2017). Rippel, Jathe, Becker, et al. (2019), found two main solving approaches: mathematical-based and simulation-based.

Mathematical approaches result in the optimal solution, for a given set of constraints. Rippel, Jathe, L'tjen, & Freitag (2019) use MILP, Mixed Integer Linear Programming, inside of a feedback loop, which is an interesting approach to consider for this report as it can handle limited accuracy of a weather forecast. Barlow et al. (2018) explore robust optimization, where they capture stochasticity with chance constraints. Irawan et al. (2017) use a bi-objective objective function which considers both the construction time and costs. Since this results in a trade-off, they use compromise programming with metaheuristics to solve. A two-stage approach combined with benders decomposition is used, by Ursavas (2017), to handle weather uncertainty. It can be noted that the meteorological conditions add a significant complexity and have to be simplified, which makes the results less realistic, but does allow for an optimization of the installation process.

Simulation allows for a more detailed representation of reality but also results in long simulation and optimization times for higher levels of aggregation (Rippel, Jathe, Becker, et al., 2019). Oelker et al. (2018) use simulation to compare the transportation of superstructures by shuttling or feedering. They find that feedering, under most circumstances, outperforms shuttling. Recent research by Tjaberings et al. (2022) is the only existing paper focusing purely on the installation of substructures, and uses in-depth simulation for different assembly strategies in combination with historical weather data. Whilst capable of realistically capturing meteorological conditions, the installation strategy has to be predefined for simulation, so no optimization is possible in this regard.

3.3 Related problems

Ksciuk et al. (2023) find that the maritime industry is not yet widely using sophisticated optimization techniques to handle uncertainty, which is why it is important to review related problems. Both Ursavas (2017) and Rippel, Jathe, L'tjen, & Freitag (2019) highlight the job shop scheduling problem (JSSP) as a related problem. Additionally, Rippel, Jathe, Becker, et al. (2019) emphasize that scheduling is an important aspect of each offshore wind farm project, which is why project scheduling problems (PSPs) are also relevant to review. As such, Section 3.3.1 explores the JSSP and Section 3.3.2 explores the PSP.

3.3.1 Job shop scheduling

Job shop scheduling considers several jobs that need to be processed in a predefined sequence by a certain set of available machines. This is similar to transportation and installation as components have to be transported and installed in a predefined sequence by the available vessels. Xiong et al. (2022) perform a literature review and classify job shop scheduling problems, of which the dynamic JSSP and JSSP with stochastic processing times are the most relevant as these approaches can be used to model weather conditions and lead times at manufacturing ports.

Mohan et al. (2019) review techniques to solve the dynamic JSSP and find that proactive reactive approaches using metaheuristics are most commonly used. This approach proactively creates a robust schedule in the first stage and then, based on the realizations, reactively updates this schedule. Proactive scheduling results in a more realistic solution than robust optimization, which assumes the worst-case scenario, and commonly uses a rolling horizon approach (Rippel, Jathe, L'tjen, & Freitag, 2019). Shahgholi Zadeh et al. (2019) explore the dynamic JSSP with variable processing times using a bee colony optimization. Sharma et al. (2023) also use bee colony to solve large-scale job shop scheduling problems.

Nouri et al. (2018) explore the flexible job shop scheduling problem and use a GA, Genetic Algorithm, as solving approach. G. Zhang et al. (2020) provide an interesting GA approach including set-up times and transportation times. Pawar & Bhosale (2022) use bee hive colonisation optimization and provide interesting visualisations. Nouiri et al. (2018) use a two-stage particle swarm optimization algorithm, which incorporates proactive scheduling.

What can be noted is that the dynamic JSSP and flexible JSSP are difficult problems to solve, since they are both NP-hard. Therefore, often meta-heuristics are used to solve these problems. Commonly used meta-heuristics are genetic algorithms and swarm-based algorithms, such as bee hive colonization and particle swarm optimization. Additionally, it can be noted that a proactive reactive approach results in a better solution quality than traditional robust scheduling. In Section 3.4, the paper by Nouiri et al. (2018) will be analyzed further due to the proactive scheduling and metaheuristic usage.

3.3.2 Project scheduling

In project scheduling, activities depend on each other in two ways. First, activities require scarce resources to be completed. Second, precedence constraints apply, which ensure a certain scheduling order. This scarcity of resources results in the resource-constrained project scheduling problem (RCPSP). For offshore wind farms, the components can be seen as the resources, whereas the precedence constraints apply to the transportation and installation. Hartmann & Briskorn (2022) review the literature on the RCPSP and distinguish between approaches. Two relevant extensions are the RCPSP with setup times and the dynamic RCPSP with either job release dates or stochastic production times. Setup times could be used to model transportation times and job release dates could be used to model production rates.

Kadri & Boctor (2018) address the RCPSP with setup times, which they consider as transfer times. They use a GA and find this efficiently solves the problem. However, they state that solving more complex test instances would be useful for future research. Gen & Lin (2023) also show that a GA is an efficient solving approach for the RCPSP with setup times.

Davari & Demeulemeester (2019) review the RCPSP with stochastic production times, whilst using Markov decision processes to model uncertainty. Tian et al. (2023) recently considered both space allocation and ordering for the RCPSP. This is an interesting approach as it can handle both production rates and port capacity. H. Zhang et al. (2024) explore a similar study to Tian et al. (2023) with the addition of uncertainty but without capacities.

In the next section, Tian et al. (2023) and H. Zhang et al. (2024) will be further analyzed for their relevant use case and uncertainty considerations respectively.

3.4 Assessing model suitability for wind turbine installation

Based on the previous sections, a selection of papers is further analysed concerning relevant model aspects for this report. This also directly answers S-RQ1 by providing a relevant selection of which models are used and what their strengths are and how these insights can be used for this report.

Four relevant model aspects are identified based on Section 2.1 and the literature reviewed in this section. Firstly, manufacturing ports each with a specific capacity and production rate. Secondly, the vessels, each with a certain speed and capacity. Moreover, it must be possible to use different transportation strategies. Thirdly, with regards to installation both the sequential

installation sequence, i.e. precedence, and operational limits must be respected in the constraints. Fourthly, concerning uncertainty, it must be possible to proactively plan for weather conditions and update decisions reactively. Table 2 shows which model aspects are considered by which paper.

Table 2: Overview of model characteristics of important literature

Aspect	Specifics	Oelker et al. (2018)	Nouiri et al. (2018)	Rippel, Jathe, L'tjen, & Freitag (2019)	Tian et al. (2023)	H. Zhang et al. (2024)
Solving	Math. model	IN	FJSS	FJSS	RCPS	RCPS
approach	Method	Simulation	2S-PSO	MILP Loop	GA	GA
Manufacturing	Multi ports	✓	✓	✓	✓	✓
	Capacity				✓	
	Production rate				✓	
Vessels	Transport times	✓	✓	✓	✓	✓
	Capacity	✓	✓	✓	✓	✓
	Multi strats	✓	✓		✓	✓
Constraints	Precedence	✓	✓	✓	✓	✓
	Operational	✓		✓		
Uncertainty	Proactive		✓	✓		✓
	Reactive			✓		
Total	**All**	**6**	**6**	**7**	**7**	**6**

Note. "Aspect" shows the modelling category and "Specifics" shows the specific characteristics. Later columns show the authors of a specific paper and include a ✓if it includes a certain characteristic. Lastly, the bottom row shows the total score, where a higher score indicates a higher suitability for this report.

Firstly, it is apparent that none of the reviewed papers meets all modelling aspects. However, it seems papers related to the RCPSP meet many of the manufacturing and vessel modelling aspects, i.e. Tian et al. (2023) and H. Zhang et al. (2024). Whereas papers related to FJSSP meet more of the uncertainty modelling aspects, i.e. Nouiri et al. (2018) and Rippel, Jathe, L'tjen, & Freitag (2019). This shows the strength of FJSS in the operational aspects and RCPSP in the manufacturing.

Secondly, only Rippel, Jathe, L'tjen, & Freitag (2019) and Oelker et al. (2018) tackle the operational constraints of wind turbine installation, as these are the only papers focused on offshore wind. This also shows these types of constraints are not common in regular FJSSP or RCPSP applications. Including these operational constraints does make modelling much more complex as the ability to perform certain jobs or activities is now weather-dependent and uncertain.

Thirdly, both Rippel, Jathe, L'tjen, & Freitag (2019) and Tian et al. (2023) achieve the highest score. Where Rippel, Jathe, L'tjen, & Freitag (2019) mainly excels in the operational uncertainty and Tian et al. (2023) in the ability to include manufacturing ports and production rates.

These findings answer S-RQ1 and illustrate that it is difficult to fully capture reality in a model. Each model has specific strengths and applications, but this knowledge can be used to develop a novel model which exploits the best features of existing models. Combining the strengths of Rippel, Jathe, L'tjen, & Freitag (2019) in the operational aspects of wind turbine installation with the ability to include manufacturing ports and production rates of Tian et al. (2023) can yield a novel approach to provide insights into the wind turbine installation process.

4 Mathematical model

This section answers S-RQ2, which looks for a realistic mathematical model based on the specific operational steps and the best modelling aspects from Section 3.4. Specifically, the mathematical formulations from Rippel, Jathe, L'tjen, & Freitag (2019) and Tian et al. (2023) are combined. As such, Section 4.1 motivates the use of a network flow model. Then, the key assumptions are motivated in Section 4.2. Next, Section 4.3 provides the notation of the model. Afterwards, the mathematical formulation is provided in Section 4.4 and verified in Section 4.5. Finally, Section 4.6 motivates why the mathematical model is realistic and thus answers S-RQ2.

4.1 Network flow model adjustments

Recall from Section 2.4 that there are three basic operational stages: manufacturing, transportation and installation. For the mathematical model, the manufacturing and installation stages are represented as single steps, but all operational steps of feedering and shuttling are kept in detail. This approach strikes a balance by simplifying independent operations, but retaining the complexity associated with the transportation strategies and thus captures the essence of the problem.

A network flow model is a logical choice as a mathematical model, as there is a natural component flow from the manufacturing ports to the offshore wind farm. Moreover, the mathematical models used by the relevant literature can all be seen as specific extensions of a network flow model. However, three adjustments have to be made to meet the specific requirements of this report.

Firstly, discrete time steps are introduced to allow for the inclusion of the weather conditions. However, the choice of time unit is important as this could come at the cost of being realistic. For example, if the chosen time unit is days, an operation that takes only 3 hours would have to be modelled as taking a full day, which could be too aggregate.

Secondly, multiple commodities are introduced. The multiple commodities represent the different components required for installation. Each vessel has a specific capacity for each component and each component takes up a certain amount of space at each port.

Thirdly, dummy nodes are introduced for each transportation vessel. In a regular network flow model, there can only be one arc from A to B, which represents a single transportation vessel. Therefore, to model multiple transportation vessels, a dummy node is introduced for each vessel, to model that there are multiple ways to get from A to B.

To illustrate these three adjustments, an example is provided for shuttling in Figure 5 and feedering in Figure 6. The arcs indicate the activities and the colour of the nodes indicates the physical location: manufacturing port (yellow), marshalling port (purple) or offshore wind site (green). For this example, consider three manufacturing ports, three components, two transportation vessels, a marshalling port and an installation vessel. In both examples, nodes 6 and 7 are the dummy nodes of the transportation vessels.

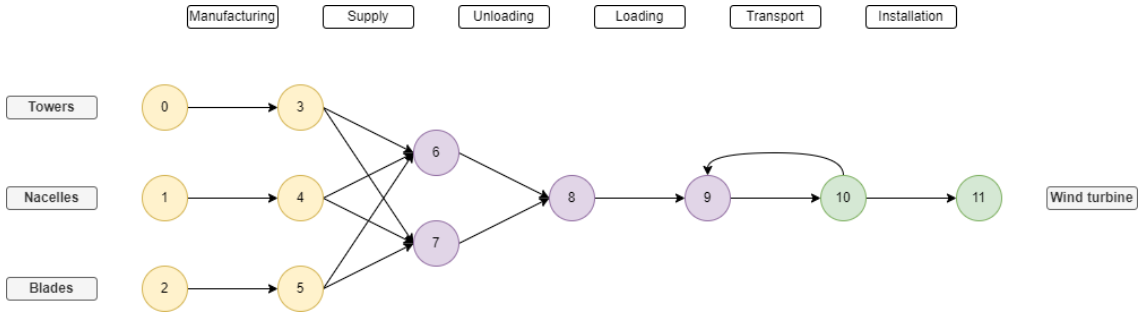

Figure 5: Network flow representation of shuttling with two transportation vessels. Activities are indicated at the top, and the colour of the nodes indicates the physical locations.

There is a clear flow of components from the source (manufacturing ports) to the sink (installation) in both figures, which visualizes why a network flow model is used. Additionally, there is a return arc from the OWF to the marshalling port (arc from node 10 to node 9) in Figure 5. For the transportation vessels, this return arc is not needed by assuming they perform a round trip from the marshalling port. The same principles hold for Figure 6. The transshipment activity requires both the installation vessel and transportation vessel to be available at the same time, implying some synchronization constraints.

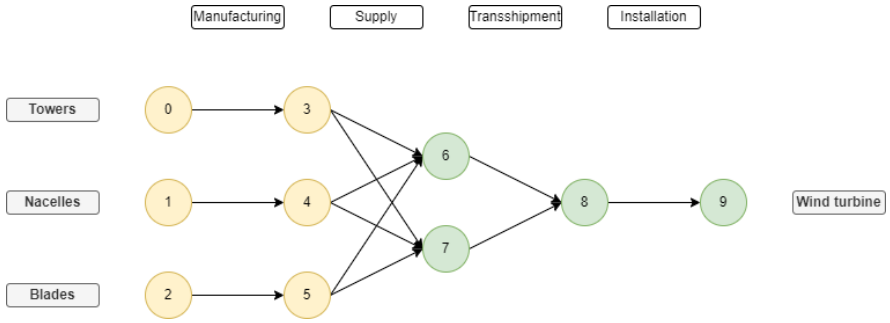

Figure 6: Network flow representation of feedering with two transportation vessels. Activities are indicated at the top, and the colour of the nodes indicates physical locations.

4.2 Assumptions

To come to a mathematical formulation, the following assumptions or simplifications are made. For each assumption, it is indicated if it is realistic or acceptable and motivated why this is the case.

1. **Fixed loading times at manufacturing ports (realistic)**
   The model considers the trip to the manufacturing port as a return arc, independently of the load. As such it is not possible to calculate the exact loading times. Therefore, a fixed loading time at the manufacturing ports, based on the capacity of the transportation vessel, is introduced. It is expected that vessels are used to full capacity since this is the most efficient method of transportation and as such is a realistic assumption.

2. **Non-weather-dependent operations can not be cancelled (Realistic)**
   Processes often can not be halted midway through an operation, e.g. it is not possible to stop manufacturing halfway through the process. Therefore, for non-weather-dependent operations, it is realistic to assume that they have to be finished once started. Logically, this also implies that for weather-dependent operations this is not the case. If operational limits are violated for weather-dependent operations, they are cancelled.

3. **Each port has a certain inventory capacity in terms of available space (Realistic)**
   The storage area is rented at a port independent of the components stored. Consequently, a port does not have a specific capacity for certain components. This assumption is also used by NSEC (2023) and is realistic.

4. **Each component takes up a fixed amount of space in a port (Realistic)**
   This is a realistic assumption as the size of the components is constant for a given project. Within this area, a factor should be included that accounts for access roads etc. This assumption is also used by NSEC (2023) and is realistic.

5. **There is a limited non-homogeneous vessel fleet available, in terms of capacity and sailing speed (Realistic)**
   The vessel fleet is limited, see Section 1, and vessels fluctuate widely in size in practice. The model can capture this variation and as such is realistic.

6. **(Un)loading takes a fixed amount of time per lift, regardless of the components lifted (Realistic)**
   The main time influence on lifting is not the lifting itself, but instead that lifting occurs, i.e. the crane has to be set up, attached to the component, the component lifted and then detached. Therefore, the component being lifted is not relevant and this assumption is realistic

7. **Each port has an unlimited number of berths for (un)loading (Acceptable)**
   In practice, it might be that there is port congestion, thus not all vessels can be handled at the same time. Whilst it would be possible to adjust the model to include a limited number of berths at a port, this is not the main interest of this study and makes the model more complex. As such, this is not considered, and this is an acceptable assumption.

8. **Vessels can indefinitely remain offshore (Acceptable)**
   Due to this assumption, the installation vessel can remain offshore under all weather conditions without having to refuel or renew the crew, which especially impacts feedering. Normally, refuelling, recrewing or storms could be reasons to return to port. But is estimated the frequency of recrewing or refuelling is low enough to not impact the results. Besides, it is possible with the use of recrew of refuel vessels. During storms, no installation is possible regardless, which is why remaining offshore under all weather conditions is also not expected to impact the results significantly. Therefore, this assumption is deemed acceptable.

4.3 Notation

In this section, the mathematical notation is introduced. Table 3 describes the relevant indices, sets, parameters and variables. Additionally, for the indices and sets, Figure 5 and Figure 6 are used to exemplify how this notation is used.

Table 3: Overview of notation of indices, sets, parameters and decision variables

Indices and sets	**Explanation**	**Figure 5**	**Figure 6**
$t \in T$	Set of time periods	0, 1,.., t^{max}	0, 1,..., t^{max}
$k \in K$	Set of all components	Tower, nacelle, blades	Tower, nacelle, blades
$i \in V$	Set of all nodes	0, 1,.., 11	0, 1,...,9
$(i,j) \in A$	Set of all arcs	(0, 3),...,(10, 11)	(0, 3),...,(8, 9)
$A_i^{Dependent} \subset A$	Set of all dependent arcs for node i	$A_6^{Dependent}$: (3, 6), (4, 6), (5, 6)	$A_6^{Dependent}$: (3, 6), (4, 6), (5, 6)
$A_{ij}^{Dependent} \subset A$	Set of all dependent arcs for arc (i,j)	$A_{3,6}^{Dependent}$: (4, 6), (5, 6), (6, 8)	$A_{3,6}^{Dependent}$: (4, 6), (5, 6), (6, 8)
$A^{Installation} \subset A$	Set of all installation arcs	(10, 11)	(8, 9)
$A^{Transport} \subset A$	Set of all transportation arcs	(9, 10)	None
$(i,j)^z \in F_+(i^t)$	Set of incoming arcs to i at time t	$F^+(3^{t+d_{03}^t})$: $(0,3)^t$	$F^+(3^{t+d_{03}^t})$: $(0,3)^t$
$(i,j)^z \in F^-(i^t)$	Set of outgoing arcs of i at time t	$F^-(3^t)$: $(3,6)^t, (3,7)^t$	$F^-(3^t)$: $(3,6)^t, (3,7)^t$
Parameters	**Explanation**	**Unit**	**Type**
c_{ij}^t	Costs to use arc (i, j) if starting in t	€	Double
c_i	Inventory costs at i	€	Double
d_{ij}^t	Time arc (i, j) is in use if starting in t	Time periods	Integer
u_{ij}^k	Capacity of arc (i,j) for component k	#components	Integer
s^k	Area component k requires	m^2	Integer
p^k	Components required for installation	#components	Integer
l_i	Available area at node i	m^2	Integer
q_i^k	Quantity of k available at i initially	#components	Integer
M	Sufficiently large number	-	Integer
Variables	**Explanation**	**When in time step**	**Type**
x_{ij}^{kt}	Flow of component k on arc (i, j)	Start	Integer
y_{ij}^t	Usage of arc (i,j)	Start	Binary
b_i^{kt}	Inventory at node i of component k	End	Integer

Note. The first column, "Indices and sets", "Parameters, "Variables", and second column, "Explanation", show the notation and its interpretation respectively. The third and fourth columns either exemplify the notation or provide units and types. Figure 5 and Figure 6 are used as examples.

4.4 Mathematical formulation

The mathematical formulation is based on Tian et al. (2023) and Rippel, Jathe, L'tjen, & Freitag (2019). Both papers use a similar formulation, but with different decision variables and constraints due to their respective application. Therefore, in this section, it will be indicated per constraint on which paper, and respective constraint in the paper, it is based. Variables x_{ij}^{kt} and y_{ij}^{t} are based on O_{lt} and x_{jt} from Tian et al. (2023) respectively. Instead of using x_{jt} with activity j being finished in time step t, y_{ij}^{t} indicates at the start of which time step arc (i,j) starts getting used. This is deliberate as now every sum in the constraints has non-negative terms but could result in times over the maximum time horizon, which is why $\min T, t + d_{ij}^{t}$ is introduced.

The objective function (1), aims to minimize the total activity and holding costs.

$$\min \sum_{i \in V} \sum_{j \in V} \sum_{t \in T} (c_{ij}^{t} * y_{ij}^{t}) + \sum_{i \in V} \sum_{k \in K} \sum_{t \in t} (c_i * b_i^{kt}) \tag{1}$$

Constraint (2): Arc usage, if there is a flow of components on arc (i, j), the arc must be used. Similar to constraint (11) from Tian et al. (2023).

$$M * y_{ij}^{t} \geq \sum_{k \in K} x_{ij}^{kt} \quad \forall (i,j) \in A, \forall t \in T \tag{2}$$

Constraint (3): Time duration, if arc (i, j) gets used at time t, it is unavailable for the next time steps for the duration d_{ij}^{t}. Based on constraint (4) from Tian et al. (2023), which refers to renewable resources. Note that if the duration of an activity is zero this constraint does not hold.

$$\sum_{z=t+1}^{z=\min t^{max}, t+d_{ij}^{t}} y_{ij}^{z} \leq 1 - y_{ij}^{t} \quad \forall (i,j) \in A, \forall t \in T \setminus t^{max} \tag{3}$$

Constraint (4): Synchronization, a vessel can only traverse one arc at the time. Based on constraint (10) from Rippel, Jathe, L'tjen, & Freitag (2019) which ensures each vessel is only involved in one operation.

$$\sum_{(m,l) \in A_{ij}^{Dependent}} \sum_{z=t}^{z=\min |T|, t+d_{ij}^{t}} y_{ml}^{z} \leq (1 - y_{ij}^{t}) * M \quad \forall (i,j) \in A, \forall t \in T \tag{4}$$

Constraint (5): Flow conservation. Based on constraints (6) and (7) from Tian et al. (2023).

$$b_i^{k,t+1} = b_i^{kt} + \sum_{(j,i)^z \in F^+(i^{t+1})} x_{ji}^{k,z} - \sum_{(i,j)^z \in F^-(i^{t+1})} x_{ij}^{k,z} \quad \forall i \in V, \forall k \in K, \forall t \in T \setminus t^{max} \tag{5}$$

Constraint (6): Arc capacity, each arc has a certain capacity per component. This custom constraint ensures vessel capacities are included. This could be seen as adjusting constraint (12) from Tian et al. (2023) to limited order size by using a maximum order size (u_{ij}^{k}) instead of M, which is a large number.

$$x_{ij}^{kt} \leq u_{ij}^{k} \quad \forall (i,j) \in A \ , \forall k \in K, \forall t \in T \tag{6}$$

Constraint (7): Inventory capacity, each site has a certain capacity in terms of space. The space all components take up combined can not exceed this. Based on constraint (9) from Tian et al. (2023).

$$\sum_{k \in K} b_i^{kt} * s_k \leq l_i \quad \forall i \in V, \forall t \in T \tag{7}$$

Constraint (8): Offshore vessel inventory, no components can be stored offshore at node i if the vessel moves towards or away from node i. Custom constraint. This can be seen as a consequence of constraint (10) from Rippel, Jathe, L'tjen, & Freitag (2019). If a vessel is only allowed to perform one operation at a time, then the vessel can not store components offshore and travel to the port at the same time.

$$\sum_{k \in K} b_i^{kt} \leq (1 - \sum_{(m,l) \in A_i^{Dependent}} y_{ml}^{t+1}) * M \quad \forall i \in V, \forall t \in T \tag{8}$$

Constraint (9): Components required for installation. Custom constraint. Rippel, Jathe, L'tjen, & Freitag (2019) enforce this implicitly by not considering separate components.

$$x_{ij}^{kt} * p^k = y_{ij}^t \quad \forall (i,j) \in A^{Installation}, \forall k \in K, \forall t \in T \setminus t^{max} \tag{9}$$

Constraint (10): Initial inventory, each location has a certain starting inventory. Custom constraint.

$$b_i^{k0} = q_i^k \quad \forall i \in V, \forall k \in K \tag{10}$$

Constraint (11): Transport arc, installation vessel must travel to OWF before it can return. Custom constraint. The plus one is there to ensure the vessel can move to the OWF initially.

$$\sum_{z=0}^{z=t} y_{ij}^z \leq \sum_{z=0}^{z=t} y_{ji}^z + 1 \quad \forall (i,j) \in A^{Transport}, \forall t \in T \tag{11}$$

Constraint (12): Return arc, installation vessel must return to port before it can move to OWF again. Custom constraint.

$$\sum_{z=0}^{z=t} y_{ji}^z \leq \sum_{z=0}^{z=t} y_{ij}^z \quad \forall (i,j) \in A^{Transport}, \forall t \in T \tag{12}$$

Constraints (13), (14), (15): Integer variables, which are also non-negative

$$x_{ij}^{kt} \in Z^+ \quad \forall (i,j) \in A \ , \forall k \in K, \forall t \in T \tag{13}$$

$$x_{ij}^{kt} \leq u_{ij}^k \quad \forall (i,j) \in A \ , \forall k \in K, \forall t \in T \tag{14}$$

$$b_i^t \in Z^+ \quad \forall i \in V \ , \forall t \in T \tag{15}$$

Constraint (16): Binary variables

$$y_{ij}^t \in \{0,1\} \quad \forall (i,j) \in A \ , \forall t \in T \ , k \in K \tag{16}$$

Overall, this formulation is a result of the formulations from Tian et al. (2023) and Rippel, Jathe, L'tjen, & Freitag (2019) with the addition of some custom constraints. This combination uses the strengths of the existing formulations which are then tailored to the specific problem in this report. This results in a multi-commodity discrete-time network flow formulation.

4.5 Model verification

Model verification checks whether the programming and implementation of the mathematical model are correct. It is impossible to fully prove the implementation is correct, but it can reasonably be shown with controlled changes of parameters (Sargent, 2010). In this subsection, these experiments are performed with small test instances, as shown in Figure 5 and Figure 6. All tests are performed on a 2.8 GHz Intel Core i7-7700HQ Quad-Core processor. The algorithms were coded in Python and run with Visual Studio Code and Gurobi as the commercial solver.

The first verification test is related to the correctness of the constraints in the model. The constraints are disabled one by one to test for undesired behaviour. If this is so, it shows the constraint is necessary for accurate modelling and that the constraint works. Table 4 shows the results of this experiment for each constraint from Section 4.4. For this experiment, unlimited space is available at each port and the rest of the parameters are set to 1, unless otherwise specified.

Table 4: Constraint and integration testing results for verification

Constraint	Specifications	Undesired behaviour	Feeder	Shuttle	Test passed
(2)		Flow, but no arcs used	Yes	Yes	Yes
(3)	$d_{ij}^t \geq 2$	Time duration one	Yes	Yes	Yes
(4)	$d_{ij}^t \geq 2$	Multiple actions	Yes	Yes	Yes
(5)		Components teleport	Yes	Yes	Yes
(6)	u_{ij}^k =1	Arc capacity exceeded	Yes	Yes	Yes
(7)	$l_i = 0$	Inventory capacity exceeded	Yes	Yes	Yes
(8)	$u_{ij}^k = 1$, $q_i^k = 2$	Floating inventory	Yes	Yes	Yes
(9)	$q_i^k = 2, q_i^{blades} = 0$	Mismatched wind turbines	Yes	Yes	Yes
(10)	$u_{ij}^k = 1$, $q_i^k = 2$	Unlimited inventories	Yes	Yes	Yes
(11) & (12)		No return trip	-	Yes	Yes

Note. The first column shows which constraint is tested. The second and third column indicates which specific adjustments were used for the test and what the undesired behaviour is. Columns four and five show if the test is passed for the feeder and shuttle instance respectively. The last column shows if the test has been passed.

Table 4 clearly shows that all constraints work as intended. Whilst these tests were only performed for relatively small dummy instances, it is reasonable to assume that these results also hold for larger instances since every key distinction was tested. The dummy instance already had multiple transportation vessels and turbines, so increasing the scale is not likely to impact the tests. Therefore, the constraints are verified and the mathematical model works as intended.

However, larger instances might have an impact on run time. With scenario testing the goal is to see how such adjustments impact run time and solution quality. Specifically, the parameters are set in such a way that it is known in advance what the optimal solution should be. In this case, this

is measured in project duration, i.e. when all wind turbines have been installed. Table 5 shows the results of this experiment. The run time was limited to 600 seconds with ports having unlimited capacity for storage, with all parameters set to 2.

Table 5: Scenario testing results for verification

H	WT	Strat	Rt (s)	Gap (%)	Strat	Rt (s)	Gap (%)
20	1	Shuttle	1.86	0.00	Feeder	0.68	0.00
20	2	Shuttle	3.09	0.00	Feeder	0.85	0.00
40	2	Shuttle	4.69	0.00	Feeder	1.60	0.00
40	4	Shuttle	90.42	0.00	Feeder	73.69	0.00
80	8	Shuttle	600	1.05	Feeder	600.00	24.00
100	10	Shuttle	600	0.79	Feeder	600.00	33.00

Note. H indicates the time horizon and WT the number of turbines to be installed. Strat indicates whether shuttling or feedering was used. Rt indicates the runtime in seconds and Gap the optimality gap in %.

Table 5 indicates that the run time seems to increase, not due to an increase in time horizon, but due to an increase in wind turbines to be installed. I.e. for $H = 40$, setting the number of turbines to four instead of two drastically increases the run time. Whereas for two wind turbines, doubling H does not even double the run time. So depending on the project size this could be a limiting factor on the usage of a commercial solver, especially since the optimality gaps increase rapidly for feedering for more than four wind turbines. Regardless, the constraint and scenario tests have shown that the model is verified and works as intended, but struggles if more wind turbines need to be installed.

4.6 Validation of the mathematical model

The proposed network flow model can fully capture the relevant operational steps, by considering manufacturing and installation as singular steps, whilst respecting the operational steps from both feedering and shuttling. The three adjustments made to the standard network flow model allow the mathematical formulation to capture all the desired characteristics of this report.

Moreover, most assumptions are validated to be realistic and only two assumptions are deemed acceptable as in Section 4.2. Whilst in the ideal scenario all assumptions would be deemed as realistic, in light of the scope of the model, the mathematical model is deemed as realistic, as no assumptions are unacceptable. This is in line with the principle that a model should be as simple as possible, but not simpler. Therefore is shown that a network flow model is a realistic representation of the relevant operations steps, which answers S-RQ2.

5 Case study

This section answers S-RQ3 and provides realistic case studies, to produce reliable results. First, Section 5.1 motivates the use of three different projects, with their respective characteristics. Second, Section 5.2 explains which operational limits apply and how this makes the planning process complex. Third, Section 5.3 dives more into the operational costs and explains why maximizing the installation rate is the same as minimizing costs as an objective. Fourthly and lastly, Section 5.4 describes the key performance indicators and ties the case studies back to S-RQ3. More details about the data gathering and choice of specific numbers can be found in Appendix A.1.

5.1 Reference projects

This section elaborates on the three reference projects and why these are relevant. In short, three projects are identified, a finished project to validate the model (NL), a currently ongoing project (DE) and a future project (DK). Figure 7 shows an overview of the project locations, the details are summarized in Table 6. The combination of these projects allows for a reliable and realistic synthesis of results, as each project uses different locations, a different WTIV and turbine size.

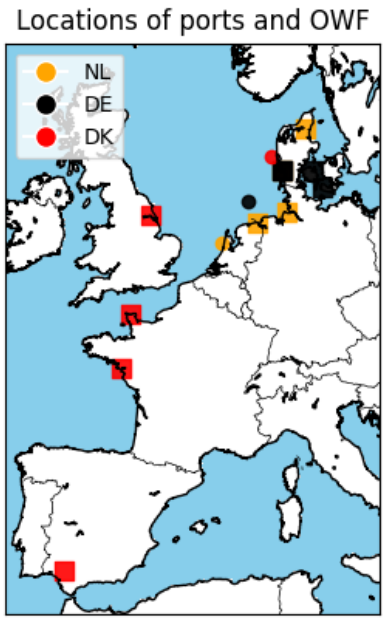

Figure 7:
Overview of project locations,
squares indicate ports,
circles indicate the OWF

Table 6: Overview of reference projects

OWF	**NL**	**DE**	**DK**
Name	HKN	Dreiht	Nordsoen
Size	0.69 GW*	0.96 GW	1.00 GW
WT size	10 MW*	15 MW	20 MW
Turbines	69	64	50
Ports	**NL**	**DE**	**DK**
Marshalling	Eemshaven	Esbjerg	Hull
Tower	Esbjerg	Esbjerg	Sevilla
Nacelle	Cuxhaven	Odense	St.-Nazaire
Blade	Aalborg	Nakskov	Cherbourg
Vessels	**NL**	**DE**	**DK**
WTIV	Scylla	Aeolus	Windpeak
WTIV speed	10.5kn	10.5kn	10.5kn
FV size	Medium	Medium	Medium
FVs	3	3	3
FV speed	14kn	14kn	14kn

Note. In bold it is highlighted which project characteristic is summarized. i.e. OWF, Ports or Vessels for each of the reference projects (NL, DE, DK).

NL is a Dutch wind farm project, the specific wind farm is Hollands Kust Noord (HKN) which was installed via shuttling. Specifically, the first turbine was installed on April 15th 2023 (Eneco, 2023) and the last turbine was installed on October 19th 2023 (CrossWind, 2023). Therefore, this project serves as a benchmark case, manufacturing and marshalling ports are the ports that were used for HKN and Scylla was also used as an installation vessel during this project. The only adjustment made for this report is that the turbine size is decreased to 10MW instead of 11MW, the number of turbines is kept at 69, highlighted by the asterisk (*).

DE is a German wind farm project, the specific wind farm is Dreiht, "It Spins" in German, an almost 1GW project which is the first to select Vestas 15MW turbines Durakovic (2021). Therefore, this project is seen as the current project. Esbjerg is the largest marshalling port (State of Green, 2022), so this is a likely suspect for shuttling since it is relatively close to Dreiht. The manufacturing ports are selected since they are close to Esbjerg and are actual manufacturing ports. Since this project uses 15MW turbines, a larger WTIV is selected, namely Aeolus.

DK is a Danish wind farm project, the specific wind farm is Nordsoen, a 1Gw project, which is still in the development stage. Therefore, this project is seen as a future project, which makes use of 20MW turbines, for which the largest WTIVs are currently being constructed (Cadeler, 2023). One such vessel is Windpeak (Cadeler, 2023), which is therefore selected as the WTIV for this project. In the future, port capacity will be limited (NSEC, 2023), which is why ports are selected which are relatively far away from the wind farm.

Logically, as the size of the wind turbines increases, the size of the components also increases. Therefore, a WTIV has less capacity for 20MW turbines than 10MW turbines. Table 7 shows the capacity of each vessel type depending on the turbine size. Additionally, the storage area required per component is summarized. The storage area for 15MW turbines is based on NSEC (2023), the rest is estimated based on the size of 10 and 20MW turbines compared to the 15MW turbine. The available storage area for each port is determined based on the report by NSEC (2023). The specific coordinates for each port and OWF, along with the port capacity are summarized in Appendix A.2.

Table 7: Vessel capacity and storage space required per wind turbine size

Vessel capacity	**10MW**	**15MW**	**20MW**	**Unit**
Scylla, FV Small	[3, 3, 9]	[2, 2, 6]	[1, 1, 3]	[Tower, Nacelle, Blade]
Aeolus, FV Medium	[5, 5, 15]	[3, 3, 9]	[2, 2, 6]	[Tower, Nacelle, Blade]
Windpeak, FV Large	[10, 10, 30]	[7, 7, 21]	[5, 5, 15]	[Tower, Nacelle, Blade]
Storage space	**10MW**	**15MW**	**20MW**	**Unit**
Tower	0.07	0.1	0.15	ha
Nacelle	0.03	0.04	0.05	ha
Blade	0.05	0.07	0.1	ha

Note. Overview of vessel capacity and storage space required depending on the turbine size

5.2 Operational limits

Weather-dependency is one of the key challenges of this report, as such it is important to realistically consider these operational limits. Installation and transshipment are the only two operations which are considered to be weather-dependent, sailing is considered outside of the scope of this report. In practice, the sailing time is also taken into account when determining a weather window, which makes the required windows much longer. However, for the scope of this report, it is assumed that vessels can be offshore under any weather conditions. Besides, sailing is possible under much worse weather conditions (Rippel, Jathe, Becker, et al., 2019), so is likely not the limiting factor on the weather windows. Additionally, as vessels sail following maritime routes, it is often possible to seek shelter in a nearby port under bad weather conditions. Therefore, it seems reasonable to not consider sailing as weather-dependent in this report and only look at installation and transshipment.

The installation steps, as illustrated in Figure 4, each have individual weather limits. Table 8 shows the different durations and weather limitations for each operation, based on installation limits from Rippel, Jathe, L'tjen, & Freitag (2019) and transshipment limits from Vis & Ursavas (2016). Jacking time includes repositioning. Additionally, Eneco (2023) shows that blade installation is possible up to 12m/s, which shows these values are perhaps more conservative than in practice. Moreover, Eneco (2023) states that a full wind turbine can be installed in less than 24 hours, which line up to the 21 hours (JU, IT, IN, IB, IB, IB, JD) following from Table 8.

Table 8: Overview of duration and operational conditions of relevant operations.

Operation	Duration (h)	Max. Wind (m/s)	Max. Wave (m)
(Un)load component (LC)	3	-	-
Transship component (TS)	3	12	2
Jack-up (JU)	3	14	2
Install tower (IT)	3	12	-
Install nacelle (IN)	3	12	-
Install blade (IB)	3	10	-
Jack-down (JD)	3	14	2

Note. "Operation" shows the operation. "Duration" shows the duration of that operation and "Max. Wind" and "Max. Wave" show the maximum allowed wind speed and wave height respectively, - means no limit. Units are indicated in brackets.

In practice, operations are only allowed to happen fully sequentially, so if the wind speed is too high for a specific operation at any point during operations, that operation is not considered possible. Moreover, often a safety factor α is applied, where there weather should be sufficiently good for an α factor of the duration. This procedure heavily restricts the opportunity for installation, which makes the planning process more complex. Sometimes this factor is also applied to the weather limits, but it is assumed these are the worst-case weather conditions, so this is unnecessary.

5.3 Operational costs

Besides the operational limits, there are also significant costs for each operation. Based on estimates from literature and company data, Table 9 summarizes the costs. It should be noted, however, that the accuracy of these costs is difficult to determine due to confidentially and lack of available data. Regardless, experts in the field have deemed that these values are in the right order of magnitude.

Table 9: Estimates of essential costs for ports and vessels

Ports	**Unit**	**10MW**	**15MW**	**20MW**
Handling	Per lift	€5,000.00	€8,000.00	€11,000.00
Holding	Per m^2/year	€100.00	€100.00	€100.00
Vessel	**Unit**	**Scylla, FV Small**	**Aeolus, FV medium**	**Windpeak, FV Large**
FV	Per day	€10,000.00	€20,000.00	€30,000.00
WTIV	Per day	€100,000.00	€200,000.00	€300,000.00

Note. "Operation" and "Unit" show the operation and corresponding unit respectively. The next three columns show these costs for a "10MW", "15MW" and "20MW" size turbine. Similarly "Vessel" indicates the vessel type and costs for increasing vessel sizes.

From Table 9 it can be derived that the handling costs are fixed for a given project as every component must be (un)loaded. In practice, port capacity is reserved such that 50% of the project turbines can be stored. Figure 8 visualizes the costs for each of the reference projects.

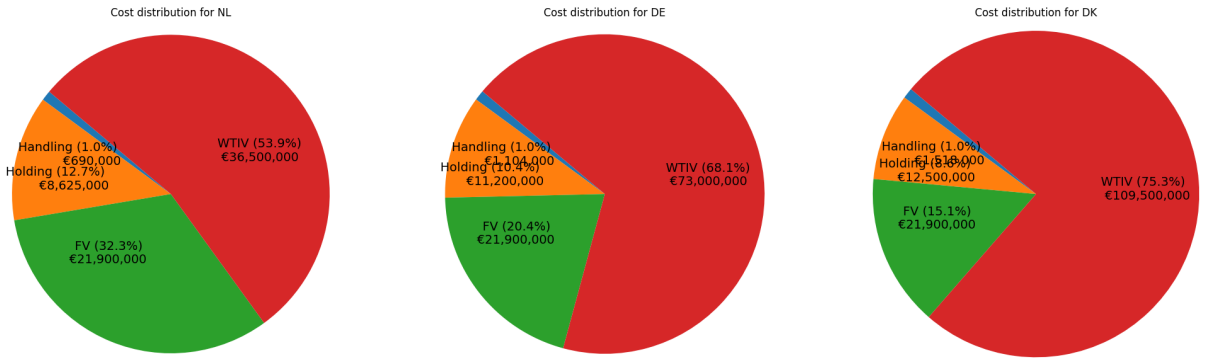

(a) NL **(b)** DE **(c)** DK

Figure 8: Visualisation of handling (blue), holding (orange), FV (green) and WTIV (red) costs

This shows that the WTIV costs comprise at least 50% and up to 75% of the total costs. Moreover, it should be noted that aspects such as port capacity and the vessel fleet are fixed for a given project once it has started. Therefore, the only method to reduce costs is to minimize the project duration, as then both port capacity and the vessels can be rented for a shorter period. Therefore, it is sufficient to maximize the installation rate for a given project, as costs will be minimized as a result.

5.4 Project evaluation and performance

To properly compare projects and different strategies some key performance indicators (KPIs) are introduced. Recall that the main indicator of interest is the installation rate. For future reference, the installation rate (I_{rate}) is defined as the number of turbines installed per day and can be calculated as:

$$I_{rate} = I_{WT}/Dur \tag{17}$$

Where I_{WT} is the number of installed turbines for a given project and Dur indicates the project duration in days. Logically, the installation rate can also be transformed in installation time (I_{time}) required per turbine. For future reference, this is defined as hours required per turbine and can be calculated as:

$$I_{time} = 24/I_{rate} \tag{18}$$

The objective of any project is to minimize costs and thus maximize the installation rate, for the reasoning behind this refer to Section 5.3. Therefore, the installation rate is an objective means to analyse the performance of a certain strategy.

However, assuming that all turbines of a project get installed, the main factor determining the installation rate is the duration of the project. Therefore, it is important to consider when each project is started. In practice, projects are often started in April (Oelker et al., 2020), as from April-October the best weather conditions occur (Rippel, Jathe, L'tjen, & Freitag, 2019). If a project is not finished within these months, installation extends to the winter, which could significantly delay the installation process. For this study that is fine, as all projects and strategies are subject to this and started at the same time. It should be noted that in practice the WTIV is often used outside of Europe in the winter months and returns during the summer months. For this report, projects are started in April 2022, unless indicated otherwise, as both 2022 and 2023 are average weather years according to Appendix C.1. This ensures that if the project runs into 2023, results are still reliable and the weather is not significantly different from 2022. Additionally, each project starts with 50% of the turbines as initial buffer, as is the standard in practice.

Provided that all projects are started at the same time and with the same initial buffer, it is possible to calculate the mean installation rate over the three projects:

$$I_{rate}^{mean} = \frac{I_{WT}^{NL} + I_{WT}^{DE} + I_{WT}^{DK}}{Dur^{NL} + Dur^{DE} + Dur^{DK}} \tag{19}$$

All in all, it can be stated that three relevant and realistic reference projects have been identified. Each project serves a different purpose and allows for interesting comparisons, and averaging over the projects results in a reliable synthesis of the results. Moreover, realistic operational limits are considered. It also has become apparent that maximizing the installation rate is the same as minimizing costs, and as such is an excellent and objective performance indicator for a certain project and strategy, as long as projects start at the same date. This will ensure the results are realistic and reliable and thus answers S-RQ3.

6 Rolling horizon simulation method

This section finds that a rolling horizon simulation method is most suitable and answers S-RQ4. First, the choice for this method is motivated in Section 6.1. Second, a conceptual model is presented in Section 6.2 that shows the in- and outputs of the model. Third, the specific weather simulation model is elaborated on in Section 6.3, which determines when weather-dependent operations are possible. Fourth, Section 6.4, based on the weather simulation results, describes the optimization method, which determines the actions to perform. Fifth, Section 6.5 describes how the updating process is performed. Sixth, Section 6.6 discusses the model limitations. Seventh and last, Section 6.7 verifies and validates the rolling horizon simulation model and answers S-RQ4.

6.1 General approach

The complexity of the problem in this report lies in the dynamic nature of weather conditions, which can only be reliable forecast for roughly two weeks (Ritchie, 2024). Therefore, it is of no use to use the model from Section 4 to solve for longer periods than that. Consequently, Rippel, Jathe, L'tjen, & Freitag (2019) use a simulation loop, similar to a rolling horizon approach, that uses simulation for weather conditions and optimization within this forecasting period. It requires simulating weather forecasts and their impact on the duration of installation or transshipment operations. This allows for the realistic inclusion of weather dependency inside the optimization model. After this simulation, an optimization model is used to create optimal vessel schedules. This in turn allows for the best possible solution for the given period and weather conditions. Therefore, especially since it is already one of the most suitable models, the approach of Rippel, Jathe, L'tjen, & Freitag (2019) is adopted for this report, as shown in Figure 9.

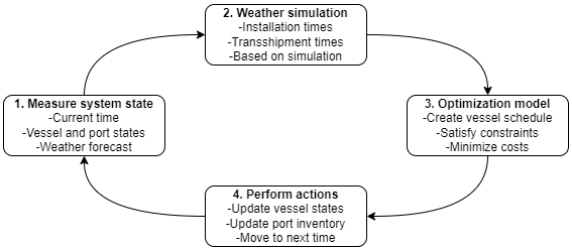

Figure 9: Rolling horizon simulation loop, based on Rippel, Jathe, L'tjen, & Freitag (2019)

In short, four steps can be distinguished in Figure 9. First, the system state is measured. This results in an overview of the vessel and port states and a weather forecast for the current time. Second, the weather forecast is used to estimate the duration of all vessel actions through simulation. Third, an optimization model is used that creates a vessel schedule, based on these action durations, for a given forecast period. Fourth, the system state is updated, as actions are performed for the current time step and the loop moves to the next time step. This loop can also be illustrated as a pseudo-algorithm, as shown in Algorithm 1 in Appendix B.1.

6.2 Conceptual model

To exemplify which data is required, in this section, a conceptual model is presented which transforms the previous steps into in- and outputs. The required data can be split into three categories: (i) System Characteristics, (ii) Historic weather data and (iii) System state. Figure 10 shows how each of these data categories provides specific inputs to the model.

System characteristics are not dynamic and fixed for the entirety of the project. The location of the OWF and operational limits are provided in the weather simulation model. Characteristics such as vessel fleet, capacity, speed, port capacity, port location and manufacturing rate are provided in the optimization model. All of these characteristics are fixed for the entire project, so these can be precomputed for every planning horizon. Historical weather data contains wind speed and wave height, which are analyzed in the weather simulation model. The system state provides the weather state, i.e. the current wind speed and wave height, to the weather simulation model for forecasting purposes. Information with regards to vessel and port states, i.e. which operation is currently being performed by a vessel or port, is provided to the optimization model.

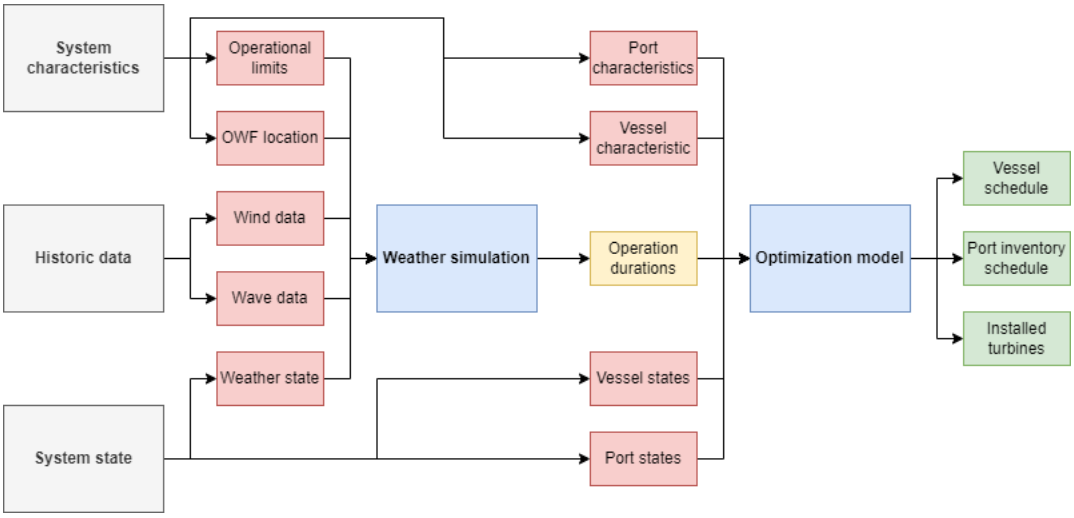

Figure 10: Overview of the conceptual model with input (red) per category (grey), output (green) and used models (blue) with intermediate results (yellow)

From Figure 10 it becomes clear that the weather simulation model is used before the optimization model and produces intermediate results. These intermediate results are then, in combination with other inputs, used in the optimization model. This results in three final outputs. Firstly, a vessel schedule, which states at which time a vessel should be performing which operation. Secondly, a port inventory schedule, which states the inventory levels at each port per time step. Thirdly and lastly, the number of installed wind turbines in this time horizon.

6.3 Markov weather simulation model

The goal of the Markov weather simulation model is to determine if a weather-dependent operation is possible, based on the inputs from Figure 10. As such, Section 6.3.1 motivates the use of a Markov model. Next, Section 6.3.2 describes the specific implementation considerations of the Markov model for this report. Lastly, Section 6.3.3 verifies and validates the model.

6.3.1 Principles

Historical data contains the historical realizations of wind speed and wave height. Because forecasting weather is a difficult process with many variables, forecasting is often bygone in literature. Instead, the historical data is taken and used as a weather forecast with 100% accuracy for simulation purposes. This approach makes it simple to estimate action durations and simulate. However, in practice, forecast accuracy rapidly decreases as the forecast period increases. For one week the accuracy is 80%, but for ten days the accuracy has already decreased to 50% (Ritchie, 2024). Therefore, it is unrealistic to assume that forecasts are 100% accurate.

Markov models are a commonly used approach to produce weather forecasts (Pandit et al., 2020) and are a relatively simple method of capturing stochasticity. Based on historical data, the probability of going from one weather condition to another can be determined. These transition probabilities are then used to produce a forecast based on the current weather. Only the current weather is relevant to determine the next weather state, the so-called memory-less property of Markov chains, so whatever weather conditions occurred in the past do not matter. This fits nicely with the rolling horizon method, where also only the current weather conditions are known.

To illustrate this approach, consider three weather states: bad, medium and good. With Markov chains, there is a certain transition probability of going from one state to another, visualized in Figure 11. Given that currently bad weather occurs, there is a $P_{B,X}$ probability of moving from the current bad weather to weather state X. Note that it is also possible to remain in a bad weather state. Additionally, the sum of the probabilities in a certain row should be 1, i.e. a next weather state must occur, as is the case in Figure 11. Note that the columns do not necessarily sum up to one, i.e. some weather conditions have a higher probability of occurring.

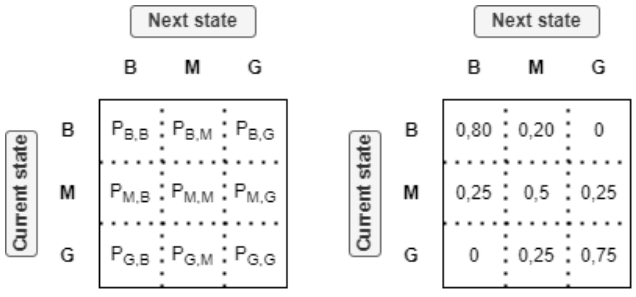

Figure 11: Probability matrix for Markov Chain, on the left with abstract probabilities, on the right with example probabilities

6.3.2 Implementation considerations

Whilst the general Markov principle is quite simple some important considerations for implementation can influence the performance. Capturing seasonality is one such consideration, if one probability matrix is used for all forecasts, there is no variation over the year, thus forecasts during summer will not be different to forecasts during winter. Therefore, to realistically capture seasonality trends, monthly probability matrices are used, similar to Pandit et al. (2020).

Additionally, Pandit et al. (2020) find a strong correlation between wave height and wind speed. This was confirmed for the OWFs in this report, with correlations of over 0.85 between wind speed and wave height. With the operational limits of this report, the wave height is only necessary for the jacking operations of the WTIV and transshipment. Whereas the wind speed is needed for every weather-dependent operation. Moreover, Ursavas (2017) state that wind speed is the limiting factor about the operational limits, not wave height.

Therefore, only wind speeds are forecast, and then the wave height is determined based on the correlation between wave height and wind speed using a simple linear regression model with intercept and coefficient. This seems like a reasonable simplification to make, especially since Table 10 shows the correlation remains roughly the same after this procedure.

Table 10: Overview of original and linearized correlation for different OWFs

OWF	Original correlation	Intercept (m)	Coefficient $(m/(m/s))$	Linearized correlation
HKN	0.8587	-0.1347	0.1712	0.8535
Dreiht	0.8563	-0.3343	0.2424	0.8536
Nord	0.8562	-0.3682	0.2402	0.8533

Note. For different OWFs the results of a linearized wave height on the correlation. The original correlation is also displayed. Intercept and coefficient are in terms of wind speed (m/s)

Another important consideration for the implementation of Markov models is the number of weather states. If too many states are considered, no historical transitions could be available, thus resulting in an infeasible model. On the other hand, if too few are considered, transitions are not captured realistically. Therefore, for this report, the considered weather states are the wind speeds rounded to integers in m/s. This strikes a good balance in terms of aggregation and fully captures the operational limits, which are also in integer m/s.

A recent report by DTN (2021) emphasized the importance of accurate weather forecasts. The key trade-off underlined is safety versus reducing costs. Where this balance lies is difficult to determine as these are difficult numbers to quantify. Therefore, a parametrized approach is proposed. To determine appropriate action durations, N simulations are performed where each simulation represents a singular forecast. Then a safety benchmark, ρ, is used to determine the appropriate duration of an activity as follows. If in ρ per cent of the simulations the activity can be completed within d time units, this is the time duration of that operation.

6.3.3 Verification and validation

To test if the discussed implementation also results in an accurate weather forecast, a verification and validation test is performed. For this test, the Markov model was trained on ERA5 hourly data from 1979-2000, and hourly data from 2000-2024 was kept separate for testing and to prevent overfitting. The test is performed for each OWF from Section 5.1 and the year 2023, which is an average year, refer to Appendix C.1 for a detailed analysis of the years 2000-2024 for each OWF.

For this test, the forecast accuracy was determined, where the number of simulations (N) and the forecast reliability (ρ) were varied. This serves as both verification and validation. Verification by reviewing the effects of N and ρ and checking if this is in line with the expectation. Validation by ensuring the forecasts are accurate enough for this report. The results of this test are visualized in Figure 12, refer to Table 19 in Appendix C.2 for the exact values.

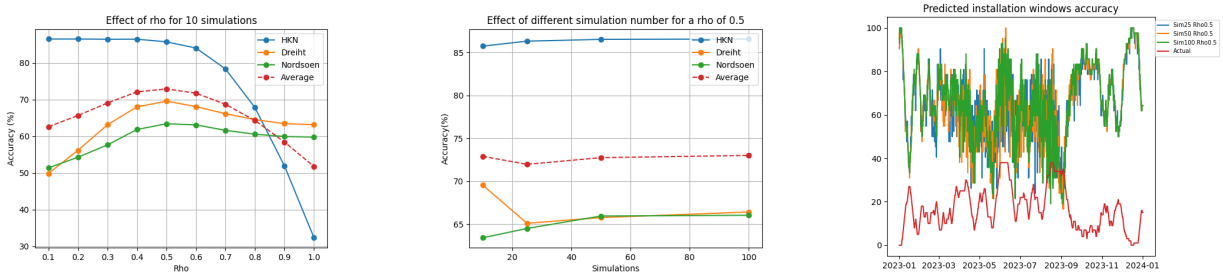

(a) Effect of different ρ values for $N = 10$

(b) Effect of increasing N if $\rho = 0.5$

(c) Dreiht: Simulation accuracy versus installation windows

Figure 12: Overview of effects of different values for ρ and N on the forecast accuracy and effect of available installation windows on the forecast accuracy respectively

Generally speaking, there seems to be an optimum for ρ around 0.5 in Figure 12a, so if half of the simulations indicate an installation window, it is accepted. This makes sense, as this strikes a balance between being overly conservative and optimistic. What is interesting to note is that accuracy is much higher for HKN than for Dreiht or Nordsoen, likely due to the better weather conditions at HKN. Interestingly, the forecast accuracy does not significantly improve for a higher number of simulations, based on Figure 12b, which indicates that 10 simulations are sufficient. Therefore, the N is set to 10 and ρ to 0.5 for the rest of this report and the model is verified.

What the forecast seems to struggle with is periods with medium weather. Figure 12c quite clearly illustrates, for Dreiht, that if the number of installation windows, the red line, is either high (42) or low (0), the forecast accuracy is high. However, if the actual number starts to hover around 20, the forecast accuracy decreases significantly. This is likely because it is easier to predict that it will remain good weather if it is already good weather. Regardless, the model achieves an average forecast accuracy of 72.92%. This validates the model since even modern forecasts are only 80% accurate for a planning horizon of a week, and 50% for 10 days (Ritchie, 2024). Therefore, the Markov model is verified and validated for this report.

6.4 Greedy optimization algorithm

This section motivates the optimization algorithm used, as this is essential in optimizing wind turbine installation. Section 4.5 shows that, for more than four wind turbines, an exact method takes over a minute to solve to optimality. Whereas real projects have to install roughly 60 turbines. Moreover, the problem is NP-hard Rippel, Jathe, L'tjen, & Freitag (2019), so for larger instances run times will explode. Consequently, a greedy algorithm is proposed, since it can generally find a good quality solution quickly, and can be used either on its own or as a starting solution for an exact method. Section 6.4.1 describes the workings of the greedy algorithm and afterwards Section 6.4.2 verifies the algorithm. Appendix C.3 contains additional numerical values of the verification.

6.4.1 Greedy algorithm

The proposed greedy algorithm is greedy in the sense that components should flow through the network as quickly as possible. The idea behind this is that the faster the components flow through the network, the quicker the turbines can be installed, thus maximizing the installation rate. In general, three steps can be distinguished: (i) Initialization, (ii) Greedy choice (iii) Feasibility check.

In the initialization of each iteration of the greedy algorithm, the current system state is used as the initial solution. This could result in certain vessels already performing an operation at the first time step. Therefore, at the start of the iteration, it is known for each arc whether or not it is active and for how long it will be unavailable if active. For this purpose, a new binary parameter is introduced: $yava_{ij}^{t}$, which indicates whether arc (i, j) is available at time t, 1 if so. If an arc is activated, $yava$ is updated not only for this arc but also for the other dependent arcs. In this way $yava$ already ensures difficult constraints, such as (3), (4) and (11), are met.

The greedy choice aspect of this algorithm lies in the arc activation and selection. As the greedy algorithm performs multiple iterations, different approaches for the arc selection are possible. The following procedure is proposed, which uses different arc orderings:

1. **First iteration: Natural:** The manufacturing arcs are checked first and the installation arc last. This ordering aims to prioritize manufacturing.
2. **Second iteration: Reversed natural:** The installation arc is checked first and the manufacturing arcs last. This ordering aims to prioritise installation if possible.
3. **Third - n/2 iterations: Random:** The arcs are shuffled and thus checked randomly. This ordering aims to avoid local optima.
4. **n/2 - final iteration: Prioritized Random:** The same principle as before, however, arcs related to the WTIV are prioritized, to stimulate installation

    - For feedering, if the WTIV has sufficient components. The installation arc is prioritized. If it is missing certain components, these transshipment arcs are prioritized.
    - For shuttling, if the WTIV is offshore and has sufficient components. The installation arc is prioritized. If not, the return arc is prioritized.

The feasibility check then only has to check a few simple constraints as *yava* already includes the difficult constraints. Once all these feasibility checks are passed, the arc can be activated and the algorithm updates *yava* and moves to the next arc in the current time step. If all arcs are checked, the algorithm moves to the next time step and the process is repeated.

Another important aspect is how the load of the arc is selected, e.g. which components to carry. In the first place, the algorithm tries to assign as many components as the arc capacity allows. However, if this violates either the inventory capacity, the loads need to be reduced. Therefore a smart load selection procedure is proposed, where components that are needed are prioritized. For example, if the WTIV is in port and already has towers and nacelles loaded, blades are prioritized. This aims to avoid inefficient loads and helps to optimize the installation rate.

Overall this algorithm aims to exploit problem-specific considerations to effectively construct a good solution. This is done by smartly incorporating difficult constraints and only checking for simple constraints, Appendix B.2 provides the pseudo-code. Moreover, specific ordering sets are used to improve the performance and ensure the algorithm does not get stuck in local optima.

6.4.2 Verification

To verify the workings of the greedy algorithm verification experiments were performed for, and averaged over, 200 iterations of the rolling horizon approach with a two-week planning horizon and time unit of 4 hours, so 84 periods. Parameters were set similarly to Section 4.5 and maritime distances are calculated using the scgraph package from MIT (Makowski, 2023).

First, the effect of the number of iterations on solution quality is tested. Increasing the number of iterations generally increases the quality of the solution. However, after 25 iterations the reduction in objective value becomes marginal, i.e. for 25 iterations this is 6.21% and for 50 iterations this is 6.35%. See Table 20 for details. At the same time, the run time doubles from 0.5 seconds for 25 iterations to 1 second for 50 iterations. Therefore, 25 iterations achieve a balance between good solution quality and an acceptable run time and show the model works as intended and is verified.

Second, the effect of the different orderings is analyzed. Table 11 shows that the full ordering increases the installation rate by 7.4% on average, which shows the orderings work as intended. However, there are significant differences between shuttling and feedering, which could be explained because shuttling has more intermediate steps, and thus benefits more from different orderings.

Table 11: Effect of different orderings on I_{rate} compared to only natural

Ordering	$I_{rate}^{shuttle}$	Diff (%)	I_{rate}^{feeder}	Diff (%)	I_{rate}^{mean}	Diff (%)
Nat	0.1623	-	0.2076	-	0.1849	-
Nat + Ran	0.1855	14.3215	0.2083	0.3371	0.1969	6.4714
Nat + Prio	0.1610	-0.7951	0.2050	-1.2763	0.1830	-1.0652
Nat + Ran + Prio	0.1914	17.9620	0.2059	-0.8171	0.1987	7.4204

Note. Diff is compared to Nat. Nat includes both Natural and reversed natural.

6.5 Update module

An essential part of a rolling horizon approach is moving to the next period and updating all the relevant variables. This section discusses the challenges and solutions for this process.

The starting point of the update module is the current state. It is known where vessels are located and whether or not they are performing an action. Port inventories are also known. So the first step of the update module is to check if any actions are finished by the next period. If they are the arcs are available again and the components transferred. If an action which is currently ongoing is unable to be finished due to bad actual weather conditions, this action is stopped and the goods are transferred to the origin. This is straightforward enough.

For the upcoming time step, new actions were decided upon. However, it is not certain that an action which was predicted to finish finished. Therefore, there might be a conflict between the current and next action. As such it is checked if the vessel is not still performing an action and is at the right location for the next action. If so, the action commences. If not the action is cancelled. This does result in undesirable situations where vessels are sitting idle since another vessel could not finish its operation. Due to the stochastic nature of weather conditions, this does represent reality where this is also not certain in advance and could happen.

Especially for feedering this is relevant. Consider that the WTIV was expected to finish the installation of a wind turbine. As such the optimization model decided that it should be loaded again in the next period. However, the installation was cancelled due to bad weather conditions and as such the inventory remains on the WTIV. As such, the loading would violate the capacity constraint and result in an infeasible model. Therefore, loading has to be cancelled and both the WTIV and feeder vessel sit idle.

To implement these actions, some adjustments to the mathematical formulation were also needed. Constraints (10), (11) and (12) had to be slightly modified in the following way:

Constraint (10): Besides initial inventory, each arc also has a starting inventory and state.

$$y_{ij}^{0} = y_{ij}^{ini} \quad \forall (i,j) \in A \tag{20}$$

$$x_{ij}^{k0} = x_{ij}^{k,ini} \quad \forall (i,j) \in A, \forall k \in K \tag{21}$$

Constraint (11): An additional binary parameter *inport* was added. Which is 1 if the vessel is in port and 0 if offshore.

$$\sum_{z=0}^{z=t} y_{ij}^{z} \leq \sum_{z=0}^{z=t} y_{ji}^{z} + 1 - inport \quad \forall (i,j) \in A^{Transport}, \forall t \in T \tag{22}$$

Constraint (12): An additional binary parameter *inport* was added. Which is 1 if the vessel is in port and 0 if offshore.

$$\sum_{z=0}^{z=t} y_{ji}^{z} \leq \sum_{z=0}^{z=t} y_{ij}^{z} + inport \quad \forall (i,j) \in A^{Transport}, \forall t \in T \tag{23}$$

6.6 Model limitations

The method in itself is very flexible, as it allows for different optimization and weather forecasting models. Moreover, a wide range of variations is possible in terms of vessel fleet, locations of OWFs and ports, production rates and weather conditions. However, some limitations apply due to the scope of this report. The key limitations of this research are: (i) vessels can remain offshore indefinitely, (ii) sailing is independent of weather conditions and (iii) port logistics are considered on an aggregate scale.

Limitations (i) and (ii) mainly relate to the weather-dependence of operations, as refuelling and recrewing can be done offshore. (i) results in vessels remaining offshore, even in storms and (ii) results in the weather forecasting model finding individual weather windows for transshipment and installation, without considering sailing. Whilst not fully realistic, both feedering and shuttling benefit from this, so it is not expected to impact the results significantly. (iii) implies that (un)loading at ports is always possible and takes a fixed amount of time. Whilst not fully realistic, this ensures the results can be attributed to the specific strategy and is not the result of port congestion.

6.7 Verification and validation

So far, all the models and modules have been verified separately. To verify and validate the rolling horizon model, the described test instances and parameter settings from Section 5.1 are used. The simulation is performed for two configurations of the optimization model. Once with the use of Gurobi (exact), with the use of the starting solution from the greedy algorithm, and once without the use of Gurobi (heur). Figure 13 shows the performance of the approaches.

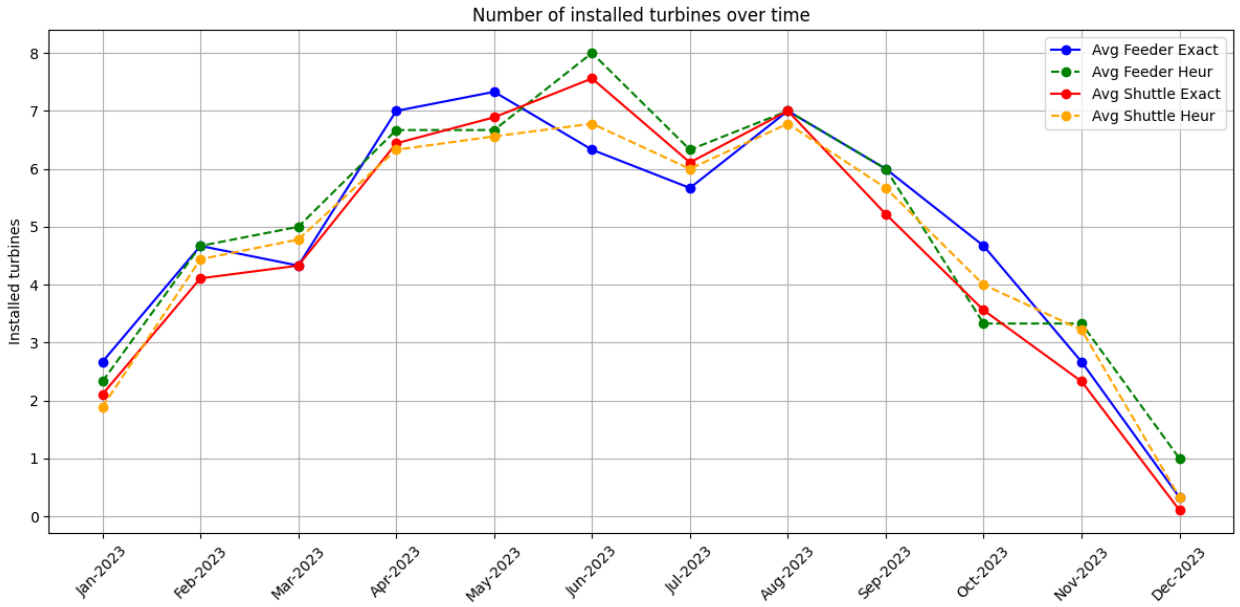

Figure 13: Overview of average installation per month for the exact and heuristic approach

Starting with the verification. It is clear to see both approaches follow the expected seasonal trends in Figure 13, i.e. more turbines are installed during the summer months. Additionally, for both approaches feedering outperforms shuttling on average. Since both approaches show the same favoured strategy and follow the seasonal trends, the rolling horizon simulation model is verified.

Interestingly enough, on average, the heuristic approach outperforms the greedy method in terms of installed turbines, refer to Table 21 for the exact values. This seems counter-intuitive because the exact method should find the optimal solution each time step for the given period. Thus resulting in a higher number of installed turbines and thus a better solution. The crux lies in the rolling horizon approach. Because, whilst the exact method might solve to optimality for each specific horizon each time step, this does not mean it solves to optimality for all time steps combined.

This still does not explain directly why the heuristic approach performs better, because these effects also apply to the greedy approach. This can likely be attributed to the nature of the solution construction in the greedy method. The greedy method aims to activate arcs as often as possible, to achieve maximal flow. This could result in a sub-optimal solution in the short term. However, in the long term, it could have beneficial effects since more components are already available. This is likely the reason why the heuristic approach performs better than the exact approach in the long term. Additionally, the run time per simulation of a full year decreases by 90% from an hour for the exact approach, to six minutes for the heuristic approach.

As for validation, the NL project serves as a benchmark project. Installation for HKN started in April 2023 and ended at the end of October 2023 using shuttling. Therefore, a simulation is also performed for the actual weather data of HKN for 2023, which allows for a realistic validation experiment. The only difficult factor is that for HKN, at times, two installation vessels were used, but is unclear for how long. To somewhat take this into account the simulation model was configured such that it started production and installation in January with no initial buffer and a single WTIV.

Simulation shows a finish date of 11-10-2023 for the NL project, roughly 9 months, where 18 turbines are installed before April. This roughly translates to using an additional WTIV for two months, which seems like a reasonable assumption, but it should be noted that no supporting evidence could be found on this assumption. This shows that the model, at the very least, is in the same order of magnitude as reality concerning installation rates and project duration and that it quite closely resembles reality if the assumption proves to be correct.

This is also the final piece of the puzzle to answer S-RQ4. First, it was motivated that a rolling horizon approach was the most realistic considering the weather uncertainty in practice, based on Rippel, Jathe, L'tjen, & Freitag (2019). Then, a Markov weather forecasting model was developed which predicts weather windows with an accuracy of 72.92%. Next, a greedy method was proposed to quickly find a good quality solution. Due to the end-of-horizon effects, this method outperformed the exact method. Lastly, the validation experiments showed that the results from the rolling horizon simulation method reasonably resemble reality and the model limitations were discussed in Section 6.6. This concludes the answer to S-RQ4.

7 Computational experiments

This section answers S-RQ5, by providing insights into the challenges in offshore wind energy. First, the setup for the experiments is discussed in Section 7.1. Next, Sections 7.2 to 7.5 contain the results of the distance, vessel size, weather and initial buffer size experiments respectively. Lastly, Section 7.6 provides managerial insights and answers S-RQ5 based on the computational results.

7.1 Experimental setup

The experimental setup is key to gaining relevant insights. Table 12 summarizes the four experiments, which ensure relevant insights can be derived. Per experiment, a full factorial approach is used, for all three reference projects and both shuttling and feedering, e.g. yielding $3 * 3 * 2 = 18$ combinations for the distance experiment. Table 13 shows the general parameter settings.

Table 12: Overview of the experimental setup

Distance	**Values**
Marshalling port	[Eemshaven, Esbjerg, Hull]
Vessel size	**Values**
WTIV	[Scylla, Aeolus, Windpeak]
FV	[Small, Medium, Large]
Weather	**Values**
Simulation year	[2003, 2015, 2023]
Alpha	[1, 1.2, 1.5]
Weather forecast	[Markov, Accurate]
Buffer size	**Values**
Production time (h)	[54, 81, 162]
Starting inventory (%)	[0-100, $\delta = 10$]

Note. Bold rows show the experiment. Non-bold shows which aspect is varied to which values for each experiment

Table 13: Parameter settings

Parameter	Value
Weather model	Markov
N	10
ρ	0.5
α	1
Forecast horizon (h)	342
Time unit (h)	9
Optimization model	Greedy
Greedy its	25
Sim start	01-04-2022
Sim end	01-01-2024

Note. Standard parameters for the simulation with values

Firstly, an experiment related to the distance between the marshalling port and the OWF is performed to see how this affects the installation rate. Secondly, an experiment related to WTIV and FV size is performed to examine if larger vessels make the installation process more efficient as theoretically less time is spent on sailing. Thirdly, an experiment related to the weather is performed to analyse how different weather conditions impact the installation rates of both strategies. Fourthly and lastly, an experiment related to buffer size is performed to check if, with sufficient starting inventory, the WTIV can be used as efficiently as possible as components are always available. With this experimental setup, all of the key aspects mentioned in Section 2.1 are tested, yielding relevant and realistic insights into the specific challenges facing offshore wind farm installation.

7.2 Distance experiment

In this section, the results of the distance experiments are discussed. Table 14 shows the finish dates for the three projects, where the marshalling port location is varied. The highest installation rate is highlighted in bold per project, which results in the shortest project duration.

Table 14: Overview of the number of installed wind turbines per project and port setup

Project	Strategy	Marshalling	D_{Mars} (km)	D^{max}_{Manu} (km)	Cap (ha)	Dur (d)	I_{rate}
NL	**Feeder**	**-**	**-**	**381.97**	**8.5**	**202.00**	**0.3416**
NL	Shuttle	Eemshaven	307.76	343.06	9.5	261.00	0.2644
NL	Shuttle	Esbjerg	500.09	203.69	9.95	283.00	0.2438
NL	Shuttle	Hull	366.08	437.98	9.87	280.00	0.2464
DE	**Feeder**	**-**	**-**	**469.28**	**13.02**	**391.00**	**0.1637**
DE	Shuttle	Eemshaven	103.96	543.26	14.56	406.00	0.1576
DE	Shuttle	Esbjerg	274.31	158.47	14.49	428.00	0.1495
DE	Shuttle	Hull	447.98	638.18	14.91	420.00	0.1524
DK	Feeder	-	-	1513.68	16.5	352.00	0.1420
DK	Shuttle	Eemshaven	416.18	1402.72	14.7	364.00	0.1374
DK	**Shuttle**	**Esbjerg**	**75.18**	**1515.03**	**13.5**	**312.00**	**0.1603**
DK	Shuttle	Hull	648.79	1351.03	14.1	343.00	0.1458

Note. The first column shows the project. The second and third column show the strategy and marshalling port. The fourth and fifth column show the distance between the OWF and marshalling port and the furthest manufacturing port to the OWF (feeder) or marshalling port (shuttle). The last three columns show the required port capacity, project duration and installation rate respectively.

Based on Table 14, on average, for the standard port configuration of each project from Section 5.1, feedering has a 9.2% higher installation rate than shuttling, whilst the required port capacity is similar. The port capacity for feedering is the sum of the three manufacturing ports, and for shuttling it is the capacity at the marshalling port. It should be noted that, generally, the best strategy in terms of installation rate also minimizes the required port capacity.

For both DE and NL, feedering is the best strategy according to Table 14, regardless of the marshalling port location for shuttling. For NL the installation rate of feedering is at least 29.2% higher than shuttling, whereas for De this is 3.8%. This is interesting as Eemshaven is located 100 km away from the OWF for DE, which is only a five-hour sail. Whereas, for feedering, the furthest manufacturing port lies almost 500 km away. Which is a 40-hour round trip. An explanation could be that this distance also has to be travelled to transport components to Eemshaven, but then the WTIV also has to travel back and forth to the port. Which adds additional time to the installation process, thus reducing efficiency. Feedering reduces project duration by two weeks for DE and almost two months for NL, which could save millions.

However, if the distance between the manufacturing ports and OWF becomes too large, shuttling becomes more attractive, as is the case for DK in Table 14. Shuttling from Esbjerg is 12.9% more efficient than feedering, saving almost 6 weeks in project duration. A big consideration still is that feedering requires no marshalling port at all. Interestingly, marshalling from Eemshaven or Hull, which are both located closer to the furthest manufacturing port, performs quite similarly to feedering. Likely due to the large distances between the marshalling port and OWF. This shows that if no marshalling port is available near the OWF, feedering can serve as a viable alternative, even if the distance between the manufacturing ports and OWF is over 1500km.

These findings are in line with Oelker et al. (2018), who also find that if the distance between the OWF and the marshalling port is too large, shuttling becomes more attractive. It should be noted that Oelker et al. (2018) only tested a 4 and 7 hours sailing time. Whereas in this report much larger sailing times, up to 60 hours, are considered. Oelker et al. (2018) find that increasing the FV fleet can render feedering more efficient, even for larger distances. This effect is confirmed for DK and Hull based on the results from Section 7.3 and Appendix D.1.

It should be noted that the difference in installation rate can not only be attributed to the distances. Both DE and DK face more challenging weather conditions than NL, which could also play a role. Figure 14 shows the installed turbines for each project over time.

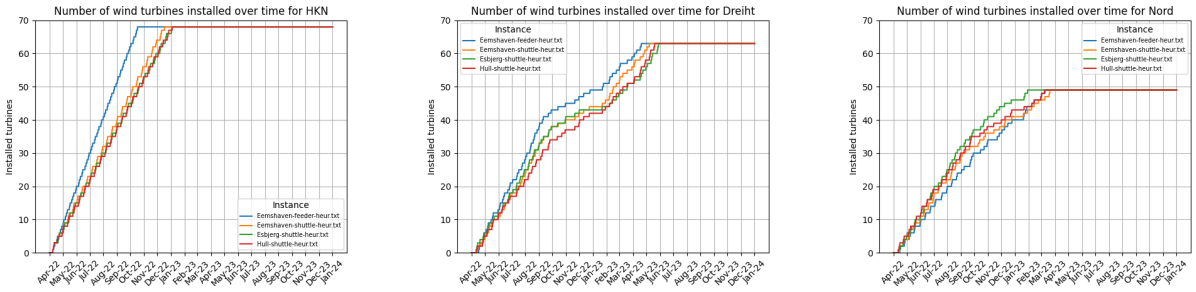

(a) NL **(b)** DE **(c)** DK

Figure 14: Visualisation of installed wind turbines over time per project

What can be observed is that installation under more difficult weather conditions, i.e. Figure 14b and Figure 14c, follows a sort of S-curve. This indicates that fewer turbines can be installed during the winter, where generally worse weather conditions occur. Whereas during the summer months weather conditions are generally better, thus resulting in a higher installation rate. Since each project starts in April with an initial buffer of 50%, each project starts with a high installation rate, but for both DE and DK, it is visible that after September the installation rate drops significantly up to March. Interestingly enough, both Figure 14 and Table 14 imply that weather conditions are not the limiting factor in feedering. For DE and DK, which both face much more difficult weather than NL, feedering is still a feasible approach. Further experiments in Section 7.4 even show that feedering is less weather-dependent than shuttling.

7.3 Vessel size experiment

In this section, the effects of the size of the FVs and WTIV are analyzed. It is expected that a larger WTIV benefits shuttling more than feedering, as the WTIV spends relatively less time sailing, whereas larger FVs impact feedering more since components are more readily available. Figure 15 visualizes the time spent on loading, sailing and installing by the WTIV per project for shuttling.

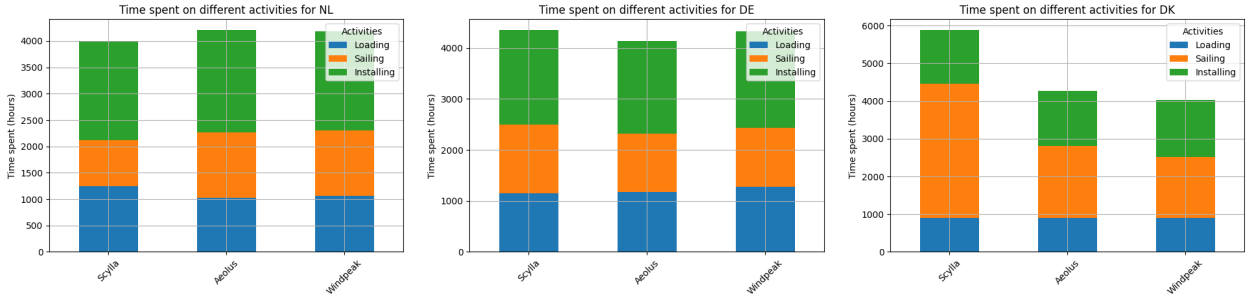

(a) NL **(b)** DE **(c)** DK

Figure 15: Time spent on loading (blue), sailing (orange) and installing (green) by WTIV for shuttling

Especially DK, and DE to a lesser extent, show the intended effect, as more time is spent on installing and less on sailing as the size of the WTIV increases. Interestingly, the expected effect does not apply to NL, which could be attributed to two factors, the end-of-horizon effect and the project itself. For NL the marshalling port is relatively nearby and Scylla can already carry three full sets, whereas for DK the marshalling port is quite far away and Scylla can only carry one full set due to the larger turbine size, which might be one reason. Additionally, end-of-horizon effects could be caused by the two-week planning horizon. This could cause the WTIV to prioritize installing one turbine in the upcoming few days over remaining in port and loading more sets to install three turbines in the upcoming weeks, thus reducing the utilisation of larger WTIVs. Even so, it remains strange that for larger WTIVs relatively more time is spent on sailing for NL.

Table 15 shows the numerical results of this experiment, averaged over the three projects, in terms of the installation rate. Consider the first three rows of Table 15, where the feeder vessels are small, and only the size of the installation vessel differs. It should first be observed that shuttling is 10-20% more efficient than feedering. For shuttling it can be observed that the installation rate generally increases for a larger WTIV. Despite the increasing size of the installation vessel, the installation rate barely changes for feedering. This could indicate that the small feeder vessels are restricting the installation rate. For feedering it is even restricting certain projects so much that they can not be finished by 2024 since the number of installed turbines is lower than 61. For shuttling every project is finished by 2024, refer to Table 22 for the extensive numerical values. This shows that if the fleet of FVs is too small, having a marshalling port speeds up the projects significantly, as the components can get consolidated there and FVs do not have to wait for transshipment offshore.

Table 15: Effect of WTIV and FV size on installation rate, averaged over the projects

WTIV	FV	Strat	I_{WT}	Dur (d)	I_{rate}	Strat	I_{WT}	Dur (d)	I_{rate}
Scylla	Small	Shuttle	61.00	382.33	0.1595	Feeder	60.00	426.67	0.1406
Aeolus	Small	Shuttle	61.00	351.00	0.1738	Feeder	60.67	424.67	0.1429
Windpeak	Small	Shuttle	61.00	359.67	0.1696	Feeder	61.00	416.33	0.1465
Scylla	Medium	Shuttle	61.00	374.00	0.1631	Feeder	61.00	363.33	0.1679
Aeolus	Medium	Shuttle	61.00	356.67	0.1710	Feeder	61.00	325.00	0.1877
Windpeak	Medium	Shuttle	61.00	363.33	0.1679	Feeder	61.00	316.67	0.1926
Scylla	Large	Shuttle	61.00	376.67	0.1619	Feeder	61.00	344.67	0.1770
Aeolus	Large	Shuttle	61.00	354.33	0.1722	Feeder	61.00	311.00	0.1961
Windpeak	Large	Shuttle	61.00	357.67	0.1705	Feeder	61.00	287.33	0.2123

Note. The first two columns indicate the WTIV and FV used. The next four columns indicate the strategy used, number of installed wind turbines, duration and installation rate. First for feedering, then for shuttling. Results are averaged over the three projects.

Now consider the next three rows, where the feeder vessel size is set to medium, the same size used for all other experiments. Interestingly, feedering now outperforms shuttling, which does confirm that the small FVs were limiting for feedering. For shuttling, the installation rate does not change significantly compared to the small FVs, which shows the small FVs were not limiting. Again, the installation rate for shuttling generally increases for a larger WTIV, but this increase is much larger for feedering, however. Using Windpeak instead of Scylla increases the installation rate by 14.7% and reduces project duration by 7 weeks on average. This effect likely occurs since larger WTIVs can serve as an offshore buffer, thus being able to install whilst the FVs are collecting components.

No consider the last three rows, where the largest feeder vessels are used. For shuttling the installation rate once again does not change significantly. For feedering however, installation rates are at least 4.5% higher than for medium feeder vessels. Additionally, larger WTIVs now drastically increase the installation rate. Using Windpeak instead of Scylla increases the installation rate by 19.9% for feedering. Reducing project duration by over 8 weeks and by a further month compared to medium feeder vessels. This results in feedering being almost 25% more efficient than shuttling.

Overall, these results are very interesting, because apparently for shuttling the size of the feeder vessels does not matter and the installation vessel only has a marginal effect on the installation rate. For feedering the feeder vessels must be sufficiently large, otherwise, the installation rate gets restricted significantly. However, if the feeder vessels are sufficiently large, the installation rate is up to 25% higher than for shuttling, resulting in 10 weeks shorter projects on average. So as long as the feeder vessels are sufficiently large, feedering generally utilizes the installation more efficiently than shuttling.

7.4 Weather experiment

In this section, the results of different years of simulation and α factors are discussed. 2003 is a good weather year, 2015 a bad weather year and 2023 an average year, see Appendix C.1 for the detailed analysis. Table 16 shows the effect on the installation rate for simulating in these years averaged over the three projects. Additionally, the value of 100% accurate forecasts is also tested. Each simulation is performed for the full year, which means projects might not finish and start in January of the respective year. See Appendix D.2 for the extensive numerical values per project.

Table 16: Effects of weather windows and simulation year on installation rate

Year	α	Strat	$I_{rate}^{forecast}$	$I_{rate}^{accurate}$	Diff (%)	Strat	$I_{rate}^{forecast}$	$I_{rate}^{accurate}$	Diff (%)
2003	1	Shuttle	0.1900	0.1959	3.12	Feeder	0.2133	0.2240	5.02
2003	1.2	Shuttle	0.1511	0.1706	12.96	Feeder	0.1551	0.1631	5.11
2003	1.5	Shuttle	0.1289	0.1563	21.28	Feeder	0.1327	0.1577	18.79
2015	1	Shuttle	0.1594	0.1796	12.70	Feeder	0.1785	0.1826	2.31
2015	1.2	Shuttle	0.1327	0.1393	4.94	Feeder	0.1329	0.1416	6.57
2015	1.5	Shuttle	0.1205	0.1366	13.39	Feeder	0.1195	0.1390	16.26
2023	1	Shuttle	0.1842	0.1918	4.13	Feeder	0.1909	0.1969	3.17
2023	1.2	Shuttle	0.1370	0.1454	6.14	Feeder	0.1452	0.1496	2.97
2023	1.5	Shuttle	0.1288	0.1438	11.69	Feeder	0.1287	0.1442	12.12

Note. The first two columns indicate the simulation year and α factor. The next four columns indicate the strategy used, total number of installed wind turbines, duration and installation rate. First for feedering, then for shuttling. Results are averaged over the three projects.

Based on the $I_{rate}^{forecast}$ from Table 16, both feedering and shuttling performed better in 2003 than in the other years due to the better weather conditions. Especially feedering performs over 10% better than in 2023 and almost 20% better than in 2015 for $\alpha = 1$. For shuttling this is only 3% for 2023 and almost 20% for 2015. Moreover, even in 2015, feedering outperforms shuttling. This is surprising as it would be expected that for worse weather conditions it becomes more difficult to transship and install offshore. This could also be explained because for shuttling the WTIV is missing installation windows during the sailing, whereas for feedering these windows can be utilized. This shows that the weather conditions do significantly impact the installation rate, but feedering suffers less from worse weather conditions.

Regardless of the installation year or forecast quality, it can be observed that the number of installed wind turbines decreases drastically for an increasing α factor. Moreover, from Table 16 it seems that the installation rates of shuttling and feedering start to converge for larger values of α. This is the case for both the Markov and accurate forecasts, but the installation rate is significantly higher for the accurate forecasts. This indicates that shuttling and feedering make use of the same weather windows and this is the limiting factor on the installation rate.

Table 16 also shows that 100% accurate forecasts improves the installation rate, $I_{rate}^{accurate}$, anywhere between 2.31% and 21.28% compared to $I_{rate}^{forecast}$, especially for higher values of α. This is not surprising, as longer weather windows are more difficult to forecast. For $\alpha = 1$ a 5.05% average increase in installation rate is observed. This means the added value of increasing the forecast accuracy is mainly interesting for larger values of α, as for $\alpha = 1.5$ the average increase is 15.59%. Interestingly, shuttling seems to benefit more from accurate forecasts, likely since the forecast has a large influence on when the WTIV sails out to install. However, even with 100% accurate forecasts, feedering remains more efficient than shuttling, be it less significant. This shows that, regardless of the forecast accuracy and simulation year, feedering is generally more efficient than shuttling.

7.5 Initial buffer experiment

In practice, projects do not start with zero initial inventory. Instead, first, a buffer of 50%, deemed as B_{trad}, is built up such that installation is not limited by component availability as there are large lead times on components (CEIF, 2022). Predictably, as the initial buffer gets larger, the required port capacity also gets larger. Figure 16 illustrates the maximum port usage for the different buffer sizes. For feedering this is the total capacity summed over the three manufacturing ports.

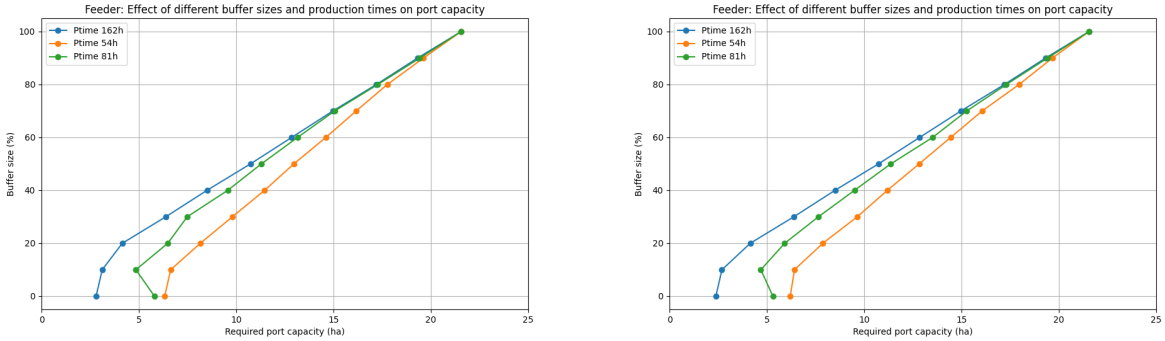

(a) Shuttle **(b)** Feeder

Figure 16: Maximum port capacity used vs initial buffer size for different production times

Two trends are observable from Figure 16. First, the required port capacity increases linearly for larger initial buffers, but at different slopes, depending on the production time. This indicates that the initial buffer size is also the largest inventory that is in the port at any point. Second, up to 20% buffer, this trend does not hold. This makes sense as 0% buffer port capacity is still required, as components still have to be stored. The same holds for 10% and 20% buffer. This means that this port capacity has to be reserved regardless, thus it might as well be filled with a 20% initial buffer as this increases the installation rate. In general, it can be noted that the required port capacity is a direct result of the production time and initial buffer size and does not depend on the strategy, as Figure 16 shows similar values for both shuttling and feedering.

Figure 17 visualizes the results of this experiment for different production rates and initial buffer sizes on the installation rate, refer to Table 24 in Appendix D.3 for the numerical values.

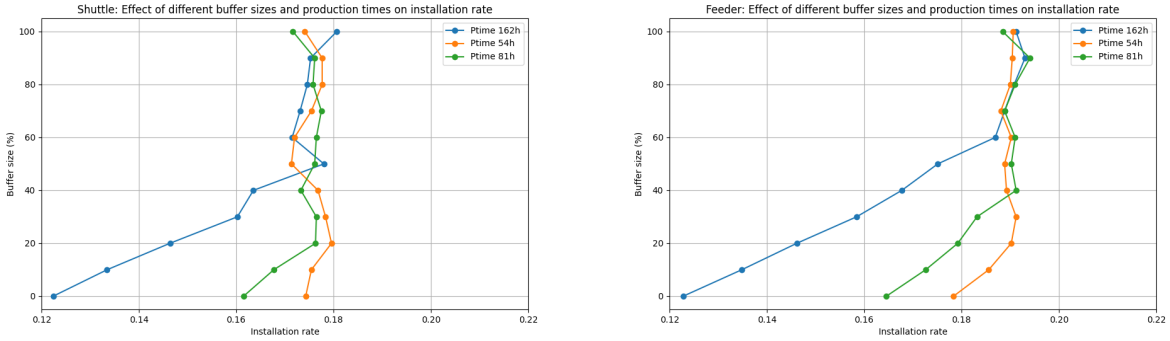

(a) Shuttle **(b)** Feeder

Figure 17: Average installation rate vs initial buffer size for different production times

Figure 17 shows two interesting trends. First, if an insufficient initial buffer is available, the installation rate gets restricted by the production time, indicated by the linear installation rate. Second, feedering requires larger buffers than shuttling, due to the higher installation rate, indicated by the line continuing longer than for shuttling. This shows there is a direct relation between the installation rate, initial buffer size and production time.

There also seems to be some noise or clutter in Figure 17, as there are variations in the installation rate, even if sufficient initial buffer is available. This is caused by the averaging over the three projects. As observed from Figure 17, the initial buffer size seems to depend on the production time and installation rate. A basic buffer size formula would be:

$$B = 1 - \frac{P_{rate}}{I_{rate}} \tag{24}$$

Where B is the buffer size and P and I are the production and unrestricted installation rate respectively. Assuming that the production rate is lower than the installation rate, otherwise, no initial buffer is required. Based on the results, the average unrestricted installation rate for feedering is roughly 0.19 turbines per day and for shuttling this is 0.17. 162 hours of production time results in a production rate of 0.15. For feedering this would mean an initial buffer of 20% and for shuttling 10%. However, based on Figure 17 this is not sufficient, for both shuttling and feedering.

The first thing to consider is that Equation (24) applies to fully linear processes where the production and installation rates are constant over time. For this problem that is not the case as the installation rate differs over time due to the weather conditions. Moreover, the installation rate defined in Section 5.4 also takes into account the time it takes from production to installation. So the manufacturing, transportation and storage times are also included, which might cause Equation (24) to not work as installation time also covers non-installation-related processes.

Therefore, a simple formula to calculate the so-called unrestricted installation time is proposed, which can be used in (24). The unrestricted installation time ($I*_{time}$) refers to the theoretical installation time if components are always available and can be calculated as:

$$I*_{time}^{Shuttle} = T^{Sailing} + T^{Loading} + \frac{T^{Install}}{W^2} \tag{25}$$

$$I*_{time}^{Feeder} = \frac{T^{Trans} + T^{Install}}{W^2} \tag{26}$$

Where $T^{Sailing}$, $T^{Loading}$, T^{Trans} and $T^{Install}$ indicate the time required for sailing, loading, transship and installing per turbine respectively. W indicates during which fraction of the year installation is possible. The weather-dependent activities are then divided by W^2 to account for the time when these activities are not possible, the square ensures a penalty for overlapping installation windows. I.e. during good weather conditions, installation can only happen after the previous installation is finished. Table 17 shows the predicted buffer size based on $I*_{time}$, B_{I*time}, the traditional 50% buffer approach, B_{trad}, and the actual required buffer size, B_{act}. The closest buffer, in terms of absolute deviation, to B_{act} is highlighted in bold.

Table 17: Overview of predicted buffer sizes and actual buffer size required

Project	P_{time} (h)	$B_{trad}^{shuttle}$	$B_{I*time}^{shuttle}$	$B_{act}^{shuttle}$	B_{trad}^{feeder}	B_{I*time}^{feeder}	B_{act}^{feeder}
NL	54.00	0.50	**0.05**	0.10	0.50	**0.25**	0.20
NL	81.00	0.50	**0.37**	0.20	**0.50**	**0.50**	0.40
NL	162.00	0.50	**0.68**	0.60	0.50	**0.75**	0.70
DE	54.00	0.50	**0.00**	0.00	0.50	**0.00**	0.10
DE	81.00	0.50	**0.00**	0.00	0.50	**0.00**	0.10
DE	162.00	0.50	**0.29**	0.20	0.50	**0.35**	0.40
DK	54.00	0.50	**0.00**	0.00	0.50	**0.00**	0.00
DK	81.00	0.50	**0.00**	0.20	0.50	**0.00**	0.00
DK	162.00	0.50	**0.28**	0.20	0.50	**0.41**	0.20

Note. For each project, production time and strategy, the predicted buffer size according to practice B_{trad} and the proposed formula $B_{I*_{time}}$ is shown, bold highlights which is closest to the actual required buffer B_{act}.

Table 17 illustrates that for all three project and production rates $B_{I*_{time}}$ is much closer to B_{act} for both shuttling and feedering. There is only one case where the same buffer size is predicted by B_{trad}, which is likely a result of chance. On average, the traditional approach deviates 0.33 from B_{act} ($MSE = 0.13$), whereas the $I * time$ approach only deviates 0.07 on average ($MSE = 0.01$). This shows the use of the traditional approach should be reconsidered as it is much too naive and robust. Therefore, the initial buffer should be calculated depending on project-dependent characteristics, as this can increase the installation rate or reduce the required port capacity depending on the project.

7.6 Managerial insights

The offshore wind expansion faces three challenges: (i) limited installation vessel fleet, (ii) limited port capacity, and (iii) operational susceptibility to weather conditions. Each challenge and the insights gained regarding this challenge are highlighted below to answer S-RQ5.

1. **Limited fleet of wind turbine installation vessels**
   Due to the limited WTIV fleet, the installation rate has to be increased significantly to meet the 2030 climate ambitions. By only starting the installation process with a certain buffer already available, the installation rate increases significantly for both shuttling and feedering, as now components are readily available for installation.

   Feedering generally increases the installation rate and reduces project duration by 9.21% compared to shuttling. This shortens project duration by 29 days on average, which could save millions. Additionally, feedering is less dependent on the quality of the weather forecast and weather conditions in general, so is also more robust than shuttling.

   Shuttling starts being more efficient than feedering if the manufacturing ports are located more than 1000 km from the OWF and the marshalling port lies within 500 km of the OWF. However, if manufacturing ports lie within roughly 500 km of the OWF, feedering is more effective. Additionally, if the size of the feeder vessels is too small, shuttling also becomes more efficient than feedering.

   This means that, in general, feedering could help significantly reduce the pressure on the limited fleet of installation vessels by increasing the installation rate by 9.21%. Additionally, it should be ensured that sufficient initial buffer is available, as this increases the installation rate for both shuttling and feedering significantly and thus also reduces the pressure on the vessel fleet, regardless of the strategy used.

2. **Limited port capacity**
   Results show that production rates have a significant impact on the required port capacity. If the production rate is 54 of 81 hours, a limited amount of port capacity is needed as just-in-time logistics can be used. However, if the production time is 162 hours per component, buffers of up to 70% of the project size could be required. This translates to roughly 20ha of storage area for a 1GW project, which might not be available in the future.

   Results also show that the required port capacity is directly related to the production time and initial buffer. Thus calculating the required initial buffer accurately will also result in the lowest amount of reserved port capacity, whilst optimizing the installation rate. Therefore, a new formula (27) to calculate the initial buffer is proposed, using the unrestricted installation time, ($I*_{time}$), instead of the 50% buffer commonly used in practice.

$$B = 1 - \frac{P_{rate}}{I*_{rate}} \tag{27}$$

The proposed formula (27) predicts the required buffer size much more closely than the traditional 50% for all projects and production times. Using the 50% is too naive and results in a significant over- or under-utilization of the port of 33pp initial buffer size, against 7pp for the proposed formula. This results in roughly 8ha against 2ha of unnecessarily reserved port capacity respectively for a 1GW project. Which shows more accurate initial buffer calculations can save hectares of required port capacity.

Since shuttling generally has a lower installation rate than feedering, it also requires less initial buffer. So if port capacity is an issue, shuttling should be considered, but this does result in a longer project duration. So whilst it might help for port capacity, it could increase the pressure on the WTIV fleet.

Additionally, increasing the production rate results in less initial buffer being required, thus alleviating the pressure on ports. Regardless, accurately determining the initial buffer required is the key to solving the port bottlenecks. Reserving the right amount of space increases the installation rate, thus reducing project duration, which helps reduce the pressure on ports.

3. **Dependence on weather conditions**

   Weather conditions play a significant role in the installation rate and project duration of offshore wind projects. Feedering, on average, performs better than shuttling in any simulated year for the nominal weather window, i.e. $\alpha = 1$. Compared to an average year, the installation rate increases by 3.1 and 11.7% for shuttling and feedering respectively in a good year. In a bad year, installation rates decrease by 13.5 and 6.5% respectively. This means that feedering benefits more from good weather and is affected less by worse weather.

   Moreover, increasing the accuracy of the weather forecast can increase the installation rate significantly. Especially for higher values of α, a more accurate weather forecast can increase the installation rate by anywhere between 11.69% and 21.28%. For $\alpha = 1$ this effect is less pronounced, as installation rates increase by 5.05% on average. Additionally, shuttling benefits much more from higher-quality forecasts, as this likely allows for a better choice of when to sail out for installation from the port.

   In general, the results show that weather dependency is indeed a significant determinant of the project duration as, depending on the simulation year, the installation rate can differ by almost 20%. However, feedering proves to be a more robust strategy than feedering, as it is affected less by different simulation years. Regardless, increasing the quality of the weather forecast can increase the installation rate anywhere between 2.31% and 21.28%, and is especially useful for shuttling or higher values of α. All in all, it is impossible to become independent of the weather conditions. However, feedering proves to be less dependent on the weather conditions than shuttling. Moreover, increasing the forecast accuracy can significantly reduce project duration in the future for both shuttling and feedering and make projects less weather-dependent.

8 Conclusion

This section provides the conclusions to this report, which looked at transportation and installation strategies for offshore wind farms with manufacturing ports. First, Section 8.1 discusses the key findings of this report and elaborates on the addressed problem. Then, Section 8.2 provides suggestions for future research. Finally, the main research question, **How do manufacturing ports, shuttling and feedering impact the installation rate?**, is answered in Section 8.3 to provide the overall conclusion of this report and can be read as a standalone section.

8.1 Key findings

European countries surrounding the North Seas have set a goal of installing at least 120 gigawatts (GW) of offshore wind energy by 2030 (NSEC, 2023). However, only 30GW is installed, which means a fourfold scale-up is required in the upcoming coming years. However, this scale-up is faced with many industry challenges (CEIF, 2022). The challenges addressed in this report are (i) a limited fleet of Wind Turbine Installation Vessels (WTIVs), (ii) bottlenecks in port capacity and (iii) weather dependency of operations, see Section 2.1 for further details.

This report uses two different wind turbine transportation and installation strategies. Shuttling, where the WTIV collects components itself at a port, and feedering, where the WTIV remains offshore and gets supplied directly via feeder vessels. The risk of shuttling is that the WTIV spends more time sailing than installing, whereas for feedering the risk is that there are insufficient weather conditions to both transship and install. Additionally, the manufacturing of components and the respective ports is of great importance to installation efficiency (Hrouga & Bostel, 2021).

Therefore, the main research question is: **How do manufacturing ports, shuttling and feedering impact the installation rate?**. To thoroughly answer the main research questions, five supporting research questions (S-RQs) are formulated, the insights of which are discussed below, which allows Section 8.3 to answer the main research question.

S-RQ1 **Which methods are currently used to optimize offshore wind farm logistics or related problems and what are their respective strengths?**

Two approaches exist: mathematical-based and simulation-based, see Section 3 for details. The strength of mathematical approaches is that they can find the optimal solution, for a given set of constraints. However, it is difficult to capture dynamic aspects of the system, such as weather conditions. This is the strength of simulation approaches, as they allow for a more detailed representation of reality, but struggle for higher levels of aggregation. In similar problems, mainly mathematical approaches are used, and heuristics are commonly used since the problems are too complex to solve otherwise. However, in these problems, the unique conditions of offshore wind farms do not apply. Therefore, combining the strong mathematical approaches of similar literature with the simulation-based approaches from problem-specific literature could yield interesting results.

S-RQ2 **How can the operational steps be translated to a realistic mathematical model?**

There are three basic operational stages: manufacturing, transportation and installation. For the mathematical model, the manufacturing and installation stages are represented as single steps, but all operational steps of feedering and shuttling are kept in detail. This approach strikes a balance by simplifying independent operations, but retaining the complexity associated with the transportation strategies and thus captures the essence of the problem.

A network flow model is a logical choice as a mathematical model, as there is a natural component flow from the manufacturing ports to the offshore wind farm. Moreover, the mathematical models used by the relevant literature can all be seen as specific extensions of a network flow model. Two key assumptions are that vessels can remain offshore indefinitely and that port congestion is not an issue. The mathematical model is thoroughly verified and all assumptions are validated in Section 4, indicating that a network flow model is a realistic mathematical model for the defined operational steps that work as intended.

S-RQ3 **Which realistic and relevant case studies can be identified for analysis?**

Three reference projects are identified, where the combination of these projects ensures the results are reliable for any application. The realism is ensured by the operational limits and cost analysis performed in Section 5. This analysis shows that minimizing costs is best achieved by maximizing the installation rate, which can be used as an objective performance indicator for each project. Therefore, these reference projects serve as a realistic case study and will ensure reliable results, as long as the starting conditions are the same.

S-RQ4 **Which method is suitable to optimize transportation and installation logistics for an offshore wind farm?**

Weather conditions can only somewhat accurately be forecast up to two weeks. As such, the strengths of a mathematical and simulation approach are combined by using a rolling horizon simulation model, which effectively captures this forecast horizon. Within this model, a Markov model makes weather forecasts, which are 72.92% accurate. The Markov weather model uses monthly transition matrices based on ERA5 data to determine if weather-dependent operations are possible, sailing is assumed to be not weather-dependent.

Then, a greedy algorithm is developed to optimize the installation rate, based on the weather forecast. To do so the greedy algorithm uses different ordering to ensure local optima are escaped. The vessel schedule following from the greedy algorithm is then applied for the next time step, and the model moves to the next time step and repeats this process. This method elaborated on in Section 6, ensures the dynamic weather conditions of the system are fully captured whilst also optimizing the installation rate, thus resulting in a suitable method to determine transportation and installation logistics for an offshore wind farm. Moreover, validation experiments show that the model, at the very least, is in the same order of magnitude as reality concerning installation rates and project duration and is therefore a suitable method.

However, there are some limitations to the model. The key assumptions are (i) vessels can remain offshore indefinitely, (ii) sailing is not weather-dependent and (iii) port logistics are considered on an aggregate scale. Whilst these limitations should be considered when studying the results, the motivation, verification and validation show the impact is limited and results are representative and realistic.

S-RQ5 **What insights can be derived regarding the challenges in offshore wind expansion?**
The offshore wind expansion faces three challenges: (i) limited installation vessel fleet, (ii) limited port capacity, and (iii) operational susceptibility to weather conditions. Experiments are set up, in Section 7, such that the location of ports, vessel size, simulation years and initial buffer size are varied. This setup ensures all key aspects impacting the industry challenges are included.

Firstly, picking the correct transportation and installation strategy can significantly enhance installation rates and reduce project durations. Feedering, on average, results in an installation rate that is 9.21% higher than shuttling and could relieve the pressure on installation vessels significantly. Secondly, accurate initial buffer calculations and increasing production rates can effectively mitigate port capacity limitations as well as increase the installation rate, having a twofold effect. Especially a new project-dependent formula proposed, performs much better than the 50% rule used in practice, as it is 26pp closer to the actual required buffer size. Lastly, improving weather forecasting reliability can increase the installation rate by 5.05% on average for nominal weather windows and especially benefits shuttling.

Combining these insights can help address the challenges in offshore wind expansion and contribute to meeting the 2030 climate goals.

8.2 Future research directions and industry recommendations

Three suggestions for future research are provided. First for for the scientific community and then for the industry as the challenges can only be addressed by progress on both ends.

First, the weather simulation could be further developed to provide more accurate forecasts, especially under medium weather conditions, and also include sailing as weather-dependent. Second, more research could be performed into negating the end-of-horizon effects for any optimization method. Third, (meta)heuristics could be further developed to handle more detailed supply chain aspects, such as port congestion, machine breakdowns, refuelling and recrewing.

For the industry first and foremost, a real-life test project should be performed using feedering, as gaining insights into the practicality of this strategy benefits future research and the industry greatly. Second, aspects such as costs, production rates and capacities should be more readily available, as this will result in future research finding more useful results. Third, more attention should be paid towards determining an initial buffer size formula, depending on project characteristics, to reserve the right amount of port capacity, as is not the case with the current 50% standard.

8.3 Overall conclusion

The installation rate of offshore wind energy has to be quadrupled by 2030 to meet the ambitious climate ambitions of European countries (NSEC, 2023). This report explores shuttling, where the WTIV collects components itself at a port, and feedering, where the WTIV remains offshore and gets supplied directly via feeder vessels. Additionally, the location of and production rate of components at the manufacturing ports are of great importance to installation efficiency (Hrouga & Bostel, 2021). Therefore, this report answers the following question: **How do manufacturing ports, shuttling and feedering impact the installation rate?**

The impact of the production rate of components at manufacturing ports is significant, as this could restrict the installation rate, resulting in the need for an initial buffer. Calculating the required initial buffer accurately either reduces the required port capacity or increases the installation rate. In practice, 50% buffer size is used as the standard. However, this report shows that this is a naive approach as it either over- or under-utilizes the reserved port capacity by 33pp initial buffer. Therefore, a new project-dependent formula (27) is proposed, resulting in a 7pp absolute deviation.

The installation rate achieved with feedering is 9.21% higher than shuttling, averaged over the three reference projects. However, if the distance between the manufacturing ports and offshore wind farm becomes too large, over 1500km in this report, shuttling is up to 12.9% more efficient. Similarly, if the size of the feeder vessels is too small, shuttling outperforms feedering by over 20%. In all other circumstances, feedering proves to be more efficient. Moreover, increasing the size of the installation vessel benefits feedering much more than shuttling, as this increases the installation rate by up to 19.9%, and only 6.4% for shuttling. Resulting in feedering having a 24.5% higher average installation rate for the largest feeder vessels and installation vessel than shuttling.

These findings are directly in line with Oelker et al. (2018), who also find that distance to the offshore wind farm and vessel capacity, number of feeder vessels in their study respectively, are the limiting factors on feedering. Simulations also show that, under different weather conditions, feedering performs consistently better than shuttling and installation rates are less affected. Additionally, increasing the quality of the weather forecast can increase the installation rate by 5.05%, on average for nominal weather windows, and especially benefits shuttling, since it is now easier to determine when to sail out. However, even with perfect information feedering outperforms shuttling.

In conclusion, the locations of manufacturing ports in combination with the production rate of components should be considered as this has a significant impact on the installation rate and which initial buffer is required. The 50% initial buffer rule used in practice is much too naive and project-dependent characteristics should be considered, as this predicts the required buffer size much more accurately. Shuttling becomes more efficient if the manufacturing ports are located far away from the offshore wind farm or if the feeder vessels are too small. In all other circumstances, feedering outperforms shuttling and is also less weather-dependent. Therefore, the industry should consider feedering as a feasible strategy to increase the installation rate and meet the 2030 climate goals, whilst keeping into account the effects of manufacturing ports.

References

Barlow, E., Öztürk, D. T., Revie, M., Akartunalı, K., Day, A. H., & Boulougouris, E. (2018). A mixed-method optimisation and simulation framework for supporting logistical decisions during offshore wind farm installations. *European Journal of Operational Research*, *264*, 894–906. Retrieved from http://dx.doi.org/10.1016/j.ejor.2017.05.043 doi: 10.1016/j.ejor.2017.05.043

Beinke, T., Ait Alla, A., & Freitag, M. (2017, 6). Resource Sharing in the Logistics of the Offshore Wind Farm Installation Process based on a Simulation Study. *International Journal of e-Navigation and Maritime Economy*, *7*, 42–54. doi: 10.1016/J.ENAVI.2017.06.005

Beinke, T., Quandt, M., Ait-Alla, A., & Freitag, M. (2020). The impact of information sharing on installation processes of offshore wind farms – Process modelling and simulation-based analysis. *International Journal of Shipping and Transport Logistics*, *12*(1-2), 92–116. doi: 10.1504/IJSTL.2020.105872

Cadeler. (2023). *Wind Peak - Cadeler.* Retrieved from https://www.cadeler.com/vessels/wind-peak

CEIF. (2022). *Ensuring the supply chain can deliver an expansion of offshore wind in Europe Recommendations to NSEC Governments-October 2022* (Tech. Rep.).

CrossWind. (2023). *CrossWind installs final wind turbine at Hollandse Kust Noord offshore wind park.* Retrieved from https://www.crosswindhkn.nl/news/2023/10/crosswind-installs-final-wind-turbine-at-hollandse-kust-noord-offshore-wind-park/

Davari, M., & Demeulemeester, E. (2019, 4). The proactive and reactive resource-constrained project scheduling problem. *Journal of Scheduling*, *22*(2), 211–237. Retrieved from https://link.springer.com/article/10.1007/s10951-017-0553-x doi: 10.1007/S10951-017-0553-X/METRICS

Drunsic, M., Ekici, D., White, M., & Gl, D. (2016, 5). Logistics and Supply-Chain Management in Offshore Wind Farm (OWF) Applications. *Proceedings of the Annual Offshore Technology Conference*, *1*, 257–265. Retrieved from https://dx-doi-org.tudelft.idm.oclc.org/10.4043/26890-MS doi: 10.4043/26890-MS

DTN. (2021). *Weather at Every Stage: How Accurate Weather Data Improves Efficiency for Offshore Wind Farms* (Tech. Rep.). Retrieved from https://www.dtn.com/wp-content/uploads/2020/07/wp_offshore_wxateverystage_0720.pdf

Durakovic, A. (2021, 7). *EnBW First to Select Vestas 15 MW Offshore Wind Turbine — Offshore Wind.* Retrieved from https://www.offshorewind.biz/2021/07/09/enbw-first-to-select-vestas-15-mw-offshore-wind-turbine/

Eneco. (2023). *Eerste turbine verrijst in offshore windpark Hollandse Kust Noord.* Retrieved from https://nieuws.eneco.nl/eerste-turbine-verrijst-in-offshore-windpark-hollandse-kust-noord/

Gen, M., & Lin, L. (2023). Genetic Algorithms and Their Applications. *Springer Handbooks*, 635–674. Retrieved from https://link.springer.com/chapter/10.1007/978-1-4471-7503-2_33 doi: 10.1007/978-1-4471-7503-2{_}33/COVER

H-Blix. (2022). H-BLIX Offshore wind vessel availability until 2030: Baltic Sea and Polish perspective-Offshore wind vessel availability until 2030: Baltic Sea and Polish perspective Final Report. Retrieved from https://windeurope.org/wp-content/uploads/files/policy/topics/offshore/Offshore-wind-vessel-avaiability-until-2030-report-june-2022.pdf

Hartmann, S., & Briskorn, D. (2022, 2). An updated survey of variants and extensions of the resource-constrained project scheduling problem. *European Journal of Operational Research*, *297*(1), 1–14. doi: 10.1016/J.EJOR.2021.05.004

Hrouga, M., & Bostel, N. (2021). Supply Chain Planning of Off-Shores Winds Farms Operations: A Review. *Lecture Notes in Mechanical Engineering*, 372–387. Retrieved from https://www.researchgate.net/publication/347191455_Supply_Chain_Planning_of_Off-Shores_Winds_Farms_Operations_A_Review doi: 10.1007/978-3-030-62199-5{_}33

Irawan, C. A., Jones, D., & Ouelhadj, D. (2017, 2). Bi-objective optimisation model for installation scheduling in offshore wind farms. *Computers & Operations Research*, *78*, 393–407. doi: 10.1016/J.COR.2015.09.010

Jiang, Z. (2021, 4). Installation of offshore wind turbines: A technical review. *Renewable and Sustainable Energy Reviews*, *139*, 110576. doi: 10.1016/J.RSER.2020.110576

Kadri, R. L., & Boctor, F. F. (2018, 3). An efficient genetic algorithm to solve the resource-constrained project scheduling problem with transfer times: The single mode case. *European Journal of Operational Research*, *265*(2), 454–462. doi: 10.1016/J.EJOR.2017.07.027

Ksciuk, J., Kuhlemann, S., Tierney, K., & Koberstein, A. (2023, 7). Uncertainty in maritime ship routing and scheduling: A Literature review. *European Journal of Operational Research*, *308*(2), 499–524. doi: 10.1016/J.EJOR.2022.08.006

Lerche, J., Lindhard, S., Enevoldsen, P., Velaayudan, A., Teizer, J., Neve, H. H., & Wandahl, S. (2022, 1). What can be learned from variability in offshore wind projects. *Energy Strategy Reviews*, *39*, 100794. doi: 10.1016/J.ESR.2021.100794

Makowski, C. (2023). *scgraph.* Retrieved from https://github.com/connor-makowski/scgraph?tab=readme-ov-file

Mohan, J., Lanka, K., & Rao, A. N. (2019, 1). A Review of Dynamic Job Shop Scheduling Techniques. *Procedia Manufacturing*, *30*, 34–39. doi: 10.1016/J.PROMFG.2019.02.006

Nouiri, M., Bekrar, A., Jemai, A., Niar, S., & Ammari, A. C. (2018, 3). An effective and distributed particle swarm optimization algorithm for flexible job-shop scheduling problem. *Journal of Intelligent Manufacturing*, *29*(3), 603–615. Retrieved from https://link.springer.com/article/10.1007/s10845-015-1039-3 doi: 10.1007/S10845-015-1039-3/METRICS

Nouri, H. E., Belkahla Driss, O., & Ghédira, K. (2018, 3). Solving the flexible job shop problem by hybrid metaheuristics-based multiagent model. *Journal of Industrial Engineering International*, *14*(1), 1–14. Retrieved from https://link.springer.com/article/10.1007/s40092-017-0204-z doi: 10.1007/S40092-017-0204-Z/FIGURES/12

NSEC. (2023). *North Seas offshore wind port study 2030 - 2050 - Final report* (Tech. Rep.).

Oelker, S., Ait-Alla, A., Lütjen, M., Lewandowski, M., Freitag, M., & Thoben, K.-D. (2018, 6). A Simulation Study of Feeder-Based Installation Concepts for Offshore Wind Farms. In *Proceedings of the twenty-eighth (2018) international ocean and polar engineering conference sapporo, japan.* OnePetro. Retrieved from https://onepetro.org/ISOPEIOPEC/proceedings-abstract/ISOPE18/All-ISOPE18/ISOPE-I-18-332/20557

Oelker, S., Alla, A. A., Büsing, S., Lütjen, M., & Freitag, M. (2020, 10). Simulative Approach for the Optimization of Logistic Processes in Offshore Ports. In *Proceedings of the thirtieth (2020) international ocean and polar engineering conference shanghai, china.* Retrieved from https://www.researchgate.net/publication/344174221_Simulative_approach_for_the_optimization_of_logistic_processes_in_offshore_ports

OffshoreWind. (2016). *CFL and Barge Master Team Up on Feeder Concept — Offshore Wind.* Retrieved from https://www.offshorewind.biz/2016/08/16/cfl-and-barge-master-team-up-on-feeder-concept/

Pandit, R. K., Kolios, A., & Infield, D. (2020, 10). Data-driven weather forecasting models performance comparison for improving offshore wind turbine availability and maintenance. *IET Renewable Power Generation*, *14*(13), 2386–2394. Retrieved from https://www.researchgate.net/publication/342202402_Data-Driven_weather_forecasting_models_performance_comparison_for_improving_offshore_wind_turbine_availability_and_maintenance doi: 10.1049/IET-RPG.2019.0941

Pawar, P. J., & Bhosale, K. C. (2022, 6). Flexible Job Shop Scheduling for Press Working Industries with Operation Precedence Constraint. *Process Integration and Optimization for Sus-*

tainability, *6*(2), 409–430. Retrieved from https://link.springer.com/article/10.1007/s41660-022-00222-w doi: 10.1007/S41660-022-00222-W/TABLES/15

Quandt, M., Beinke, T., Ait-Alla, A., & Freitag, M. (2017). Simulation Based Investigation of the Impact of Information Sharing on the Offshore Wind Farm Installation Process. *Journal of Renewable Energy*, *2017*, 1–11. doi: 10.1155/2017/8301316

Rippel, D., Jathe, N., Becker, M., Lütjen, M., Szczerbicka, H., & Freitag, M. (2019, 1). A Review on the Planning Problem for the Installation of Offshore Wind Farms. *IFAC-PapersOnLine*, *52*(13), 1337–1342. doi: 10.1016/J.IFACOL.2019.11.384

Rippel, D., Jathe, N., L'tjen, M., & Freitag, M. (2019, 11). Evaluation of Loading Bay Restrictions for the Installation of Offshore Wind Farms Using a Combination of Mixed-Integer Linear Programming and Model Predictive Control. *Applied Sciences 2019, Vol. 9, Page 5030*, *9*(23), 5030. Retrieved from https://www.mdpi.com/2076-3417/9/23/5030 doi: 10.3390/APP9235030

Ritchie, H. (2024). Weather forecasts have become much more accurate; we now need to make them available to everyone. *Our World in Data*. Retrieved from https://ourworldindata.org/weather-forecasts

Sargent, R. G. (2010). Verification and validation of simulation models. *Proceedings - Winter Simulation Conference*, 166–183. Retrieved from https://www.researchgate.net/publication/224209154_Verification_and_validation_of_simulation_models doi: 10.1109/WSC.2010.5679166

Sarker, B. R., & Faiz, T. I. (2017, 2). Minimizing transportation and installation costs for turbines in offshore wind farms. *Renewable Energy*, *101*, 667–679. doi: 10.1016/J.RENENE.2016.09.014

Shahgholi Zadeh, M., Katebi, Y., & Doniavi, A. (2019, 5). A heuristic model for dynamic flexible job shop scheduling problem considering variable processing times. *International Journal of Production Research*, *57*(10), 3020–3035. Retrieved from https://www.tandfonline.com/doi/abs/10.1080/00207543.2018.1524165 doi: 10.1080/00207543.2018.1524165

Sharma, N., Sharma, H., & Sharma, A. (2023, 9). Thermal Artificial Bee Colony Algorithm for Large Scale Job Shop Scheduling Problems. *SN Computer Science*, *4*(5), 1–15. Retrieved from https://link.springer.com/article/10.1007/s42979-023-02141-0 doi: 10.1007/S42979-023-02141-0/METRICS

State of Green. (2022). *Port of Esbjerg: World's largest base port for offshore wind activities*. Retrieved from https://stateofgreen.com/en/news/port-of-esbjerg-worlds-largest-base-port-for-offshore-wind-activities/

Tian, B., Zhang, J., Demeulemeester, E., Chen, Z., & Ali, H. (2023, 11). Integrated resource-constrained project scheduling and material ordering problem considering storage space allocation. *Computers & Industrial Engineering*, *185*, 109608. doi: 10.1016/J.CIE.2023.109608

Tjaberings, J., Fazi, S., & Ursavas, E. (2022, 12). Evaluating operational strategies for the installation of offshore wind turbine substructures. *Renewable and Sustainable Energy Reviews*, *170*, 112951. doi: 10.1016/J.RSER.2022.112951

Ursavas, E. (2017, 4). A benders decomposition approach for solving the offshore wind farm installation planning at the North Sea. *European Journal of Operational Research*, *258*(2), 703–714. doi: 10.1016/J.EJOR.2016.08.057

Van Oord. (n.d.). *Offshore wind installatieschip — Van Oord.* Retrieved from https://www.vanoord.com/nl/materieel/offshore-wind-installatieschip/

Van Oord. (2020). *Aeolus voltooit installatie turbines bij Borssele III & IV — Van Oord.* Retrieved from https://www.vanoord.com/nl/updates/aeolus-voltooit-installatie-turbines-bij-borssele-iii-iv/

Vis, I. F., & Ursavas, E. (2016, 4). Assessment approaches to logistics for offshore wind energy installation. *Sustainable Energy Technologies and Assessments*, *14*, 80–91. doi: 10.1016/J.SETA.2016.02.001

Xiong, H., Shi, S., Ren, D., & Hu, J. (2022, 6). A survey of job shop scheduling problem: The types and models. *Computers & Operations Research*, *142*, 105731. doi: 10.1016/J.COR.2022.105731

Zhang, G., Hu, Y., Sun, J., & Zhang, W. (2020, 5). An improved genetic algorithm for the flexible job shop scheduling problem with multiple time constraints. *Swarm and Evolutionary Computation*, *54*, 100664. doi: 10.1016/J.SWEVO.2020.100664

Zhang, H., Ma, R., & He, Z. (2024, 1). Project scheduling cost optimization based on resource transfer costs and robustness. *Computers & Operations Research*, *161*, 106445. doi: 10.1016/J.COR.2023.106445

A Case study details

This section contains more details about the reference projects. Appendix A.1 provides more details about the data gathering. Appendix A.2 contains the locations of the different port, including the capacity according to NSEC (2023), and the offshore wind farms.

A.1 Port and vessel details

All the ports and OWFs considered in Table 6 are real locations. Moreover, based on search results all the manufacturing ports do also produce the components for which they are chosen in this report. It is not considered to which company, e.g. Vestas or Siemens, they belong and wether or not this would make a difference. The 10.5kn speed for the WTIVs is based on the technical leaflet of Aeolus (Van Oord, n.d.). The 14kn speed for the FVs is based on OffshoreWind (2016), which goes into detail about FVs specifically designed for offshore wind farms. These FVs are able to remain stable under offshore weather conditions. The speed is also in line with the 12kn speed from Tjaberings et al. (2022). The capacity of the FVs is set equal to the WTIVs, but it should be noted that the FVs only transport one type of component.

Scylla is a logical choice for a WTIV as it was used for HKN (Eneco, 2023), moreover the WTIV can clearly carry at most three sets, one set consists of tower, nacelle and three blades, of components for the 11MW turbine, which is why this capacity is chosen in Table 7. It is assumed that it can carry two 15MW sets and singular 20MW set.

Windpeak is also an obvious choice as this is the largest WTIV currently being developed (Cadeler, 2023). Cadeler (2023) states the WTIV can carry seven 15MW sets and five 20MW sets. The 10MW capacity is extrapolated to 10 10MW sets in Table 7.

Aeolus is chosen such that is somewhat in between Windpeak and Scylla. The capacity is hypothetical, but based on (Van Oord, 2020) the vessel is capable of carrying at least 4 sets, but it is unknown what size of turbines it is. Therefore, it is assumed Aeolus can carry 5 sets of 10MW turbines, 3 of 10MW and 2 of 20MW.

The storage area for the 15MW the space is based on NSEC (2023). Based on company experts, it seems the required space for a 1GW project remains somewhat constant, regardless of the turbine size. Which is why a 10MW takes up 0.25ha and a 20MW turbine takes up 0.5ha in total. This results in 25ha for a 1GW project, which is roughly the same as the 23.45ha for 15MW turbines.

A wide variation of costs is used in literature. Based on Oelker et al. (2018) FVs cost between €10,000 and €20,000 a day and WTIV costs roughly 10 times as much. Since this is a somewhat dated paper, the 10k is considered for the small FVs, the 20k for the medium FVs and 30k is extrapolated for large FVs. Similarly, 100k per day is considered for small WTIVs, Scylla, 200k for medium WTIVs, Aeolus, and 300k for large WTIVs, Windpeak. The port costs are confidential and based on estimates from company experts.

A.2 Locations

Table 18 contains the locations of the different ports and offshore wind farms used in this report.

Table 18: Overview of locations (latitude and longitude) of the different ports and OWFs

Location	Latitude	Longitude	Capacity (ha)
Aalborg	57.0473254	10.05225162	160
Cuxhaven	53.84383512	8.751225665	22
Eemshaven	53.45623339	6.814810008	40
Esbjerg	55.45631922	8.469560422	160
Hull	53.74461035	-0.304458825	40
Odense	55.46741202	10.5380936	70
Nakskov	54.82949054	11.12208984	60
Sevilla	37.34283264	-5.999056323	20
HKN	52.61725275	4.428005129	-
Dreiht	54.31396122	6.223031007	-
Nordsoen	55.982962962	7.742442031	-
Cherbourg	49.6655402	-1.62626	100
Saint-Nazaire	47.254742	-2.2210268	13

Note. Shows the latitude and longitude of each of the different ports and OWFs used in this report.

B Pseudo-codes

This section contains the pseudo-codes of the rolling horizon loop, Appendix B.1, and the greedy algorithm, Appendix B.2.

B.1 Rolling horizon algorithm

Algorithm 1 Decision making algorithm

```
System Initialization
T = 0
ΔT = timestep
while T < SimDuration do
    Measure system state
    if all wind turbines installed then
        stop
    Run weather simulation model
    Run optimization model
    Update system state
    T = T + ΔT
```

Algorithm 1 illustrates the steps of Figure 9 in an algorithm form. In short, the algorithm consists of a single while loop. There are two stopping criteria, either the maximum simulation time is met ($SimDuration$) or all wind turbines are installed.

B.2 Greedy algorithm

Algorithm 2 Greedy Method

```
1: procedure GreedyMethod
2:     Initialize system state as initial solution
3:     for t = 1 to T do                                   ▷ Loop over time steps
4:         for all arcs (i, j) do
5:             Calculate y_ij^av indicating if arc (i, j) is available at time t
6:         for iter = 1 to n do                            ▷ Loop over iterations
7:             if iter = 1 then                            ▷ First iteration: Natural order
8:                 Sort arcs in natural order (manufacturing to installation)
9:             else if iter = 2 then                       ▷ Second iteration: Reversed natural order
10:                Sort arcs in reversed natural order (installation to manufacturing)
11:            else if iter > 2 and iter ≤ n/2 then        ▷ Random order
12:                Randomly shuffle arcs
13:            else                                        ▷ Prioritized WTIV order
14:                Randomly shuffle arcs prioritizing WTIV-related arcs
15:            for all arcs (i, j) do
16:                if arc is active and available then
17:                    Update y_ij^av for this arc and dependent arcs
18:                    Perform feasibility check for arc (i, j)
19:                    if feasible then
20:                        Activate arc (i, j)
21: procedure FeasibilityCheck(i, j)
22:    Determine load of arc (i, j)
23:    if load violates loading capacity or inventory capacity then
24:        Reduce load to satisfy constraints
```

Algorithm 2 describes the inner workings of the greedy algorithm. Specifically it shows how the arcs are ordered and activated if feasible.

C Extensive verification and validation results

This section contains the extensive results of the validation and verification experiments. Appendix C.1 contains the analysis of the yearly installation windows. Next, Appendix C.2 contains the forecast accuracy for each reference project depending on N and ρ. Afterwards, Appendix C.3 expands on the performance of the greedy and exact optimization method.

C.1 Yearly installation hours

First, the number of available installation hours for the years 2000 up to 2024 are determined based on the historical data, Figure 18 shows the number of hours in which installation was possible. This means a maximum of roughly $365 * 24 = 8760$ hours of installation is possible under perfect weather conditions. Figure 18 shows the number of hours that installation is possible each year, for different values for the safety factor α ([1, 1.2, 1.5]). Recall that α increases the required duration of the installation windows, likely resulting in fewer available installation hours for higher values of α.

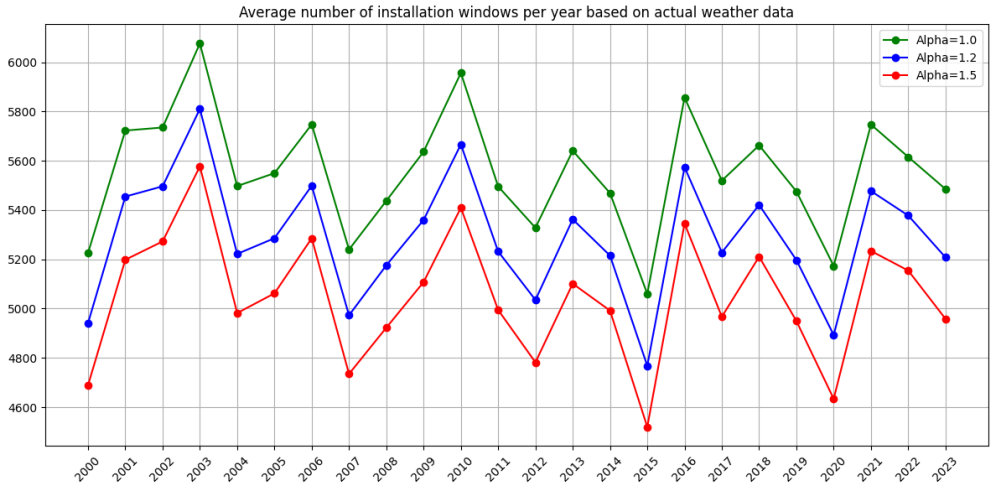

Figure 18: Average number of installation windows over the years for the years 2000 up to 2024

What should be observed is that there are large fluctuations in the number of installation hours over the years. From the data, three key years were identified: 2003, 2015 and 2023. In 2003 the highest number of installation hours occurred, whereas in 2015 the least number of installation hours occurred. Lastly, 2023 was chosen since it closely resembles the mean number of installation hours, thus deeming it as an average year. 2022 also quite closely resembles the mean, which means running simulations from 2022-2024, represents average years. Therefore, this is a good choice for the experiments, as it represents average weather conditions and includes the designated average year.

C.2 Forecast accuracy

Table 19 shows the full table of forecast accuracy's.

Table 19: Overview of forecast accuracy in 2023 for a given number of simulations and accuracy factor

N	ρ	HKN (%)	Dreiht (%)	Nord (%)	Mean (%)
1	1	74.51	62.85	59.62	65.66
3	0.3	86.04	58.83	56.55	67.14
3	0.6	80.79	65.93	60.79	69.17
3	1	58.21	64.59	60.76	61.19
5	0.2	86.44	55.47	54.18	65.36
5	0.4	86.12	63.76	59.03	69.64
5	0.6	83.03	67.29	61.82	70.71
5	0.8	70.79	66.03	61.59	66.14
5	1	46.99	63.86	60.33	57.06
10	0.1	86.53	49.84	51.38	62.58
10	0.2	86.53	56.17	54.28	65.66
10	0.3	86.47	63.12	57.64	69.08
10	0.4	86.48	68.02	61.84	72.11
10	**0.5**	**85.76**	**69.58**	**63.42**	**72.92**
10	0.6	84.07	68.10	63.10	71.75
10	0.7	78.36	66.15	61.62	68.71
10	0.8	67.80	64.56	60.56	64.31
10	0.9	51.88	63.44	59.94	58.42
10	1	32.30	63.16	59.76	51.74
25	0.5	86.34	65.11	64.51	71.99
50	0.5	86.55	65.78	65.96	72.76
100	0.5	86.59	66.43	66.05	73.02

Note. The higher simulation runs (25+) were performed after the initial rho and simulation experiments for run time purposes

C.3 Performance of greedy and exact optimization model

Table 20 shows the effect of more iterations on the greedy algorithm solution quality.

Table 20: Effect of number of iterations on solution quality and run time for feedering strategy

Iterations	Objective value	Reduction (%)	Runtime (s)	Rt/it (s)
1	-974218	0.00	0.032	0.032
10	-1028850	5.61	0.224	0.0224
25	-1034672	6.21	0.497	0.01988
50	-1036106	6.35	0.931	0.01862
100	-1037017	6.45	1.785	0.01785

Note. The first column shows the number of iterations. The second and third column shows the objective value and relative reduction compared 1 iteration. The fourth and fifth column show the total run time and run time per iteration respectively.

Table 21 shows the difference in project duration and installed wind turbines between the heuristic and exact method, which uses the heuristic solution as the starting solution.

Table 21: Number of turbines that were installed, on average, for the exact and heuristic approach.

Strategy	I_{WT}^{exact}	I_{WT}^{heur}	I_{WT}^{diff}	Duration diff (days)
Feeder	58.67	60.33	1.67	-8.75
Shuttle	55.78	56.78	1.00	-3.04
Average	57.22	58.56	1.33	-5.90

Note. The first column shows the strategy. The second and third column show the number of installed turbines for both approaches. Columns four and five show the difference first in turbines then in average project duration.

D Extensive computational results

This section provides extensive results of the computational experiments. Appendix D.1 provides the full results of the vessel size experiment. Then, Appendix D.2 does the same for the weather experiments. Lastly, the numerical results of the buffer experiment are provided in Appendix D.3.

D.1 Vessel size experiment

Table 22: Overview of effects of different vessels for each reference project

Project	Strat	WTIV	FV	I_{WT}	Dur (d)	I_{rate}
DE	feeder	Aeolus	Large	64	402	0.159204
DE	shuttle	Aeolus	Large	64	409	0.1564792
DE	feeder	Aeolus	Medium	64	403	0.1588089
DE	shuttle	Aeolus	Medium	64	430	0.1488372
DE	feeder	Aeolus	Small	64	420	0.152381
DE	shuttle	Aeolus	Small	64	419	0.1527446
DE	feeder	Scylla	Large	64	412	0.1553398
DE	shuttle	Scylla	Large	64	430	0.1488372
DE	feeder	Scylla	Medium	64	442	0.1447964
DE	shuttle	Scylla	Medium	64	428	0.1495327
DE	feeder	Scylla	Small	64	429	0.1491841
DE	shuttle	Scylla	Small	64	439	0.1457859
DE	feeder	Windpeak	Large	64	403	0.1588089
DE	shuttle	Windpeak	Large	64	438	0.1461187
DE	feeder	Windpeak	Medium	64	378	0.1693122
DE	shuttle	Windpeak	Medium	64	439	0.1457859
DE	feeder	Windpeak	Small	64	413	0.1549637
DE	shuttle	Windpeak	Small	64	439	0.1457859
NL	feeder	Aeolus	Large	69	203	0.3399015
NL	shuttle	Aeolus	Large	69	283	0.2438163
NL	feeder	Aeolus	Medium	69	202	0.3415842
NL	shuttle	Aeolus	Medium	69	277	0.2490975
NL	feeder	Aeolus	Small	69	214	0.3224299
NL	shuttle	Aeolus	Small	69	282	0.2446809
NL	feeder	Scylla	Large	69	210	0.3285714
NL	shuttle	Scylla	Large	69	265	0.2603774
NL	feeder	Scylla	Medium	69	202	0.3415842
NL	shuttle	Scylla	Medium	69	265	0.2603774

NL	feeder	Scylla	Small	69	211	0.3270142
NL	shuttle	Scylla	Small	69	266	0.2593985
NL	feeder	Windpeak	Large	69	200	0.345
NL	shuttle	Windpeak	Large	69	283	0.2438163
NL	feeder	Windpeak	Medium	69	205	0.3365854
NL	shuttle	Windpeak	Medium	69	282	0.2446809
NL	feeder	Windpeak	Small	69	213	0.3239437
NL	shuttle	Windpeak	Small	69	276	0.25
DK	feeder	Aeolus	Large	50	328	0.152439
DK	shuttle	Aeolus	Large	50	371	0.1347709
DK	feeder	Aeolus	Medium	50	370	0.1351351
DK	shuttle	Aeolus	Medium	50	363	0.137741
DK	feeder	Aeolus	Small	49	640	0.0765625
DK	shuttle	Aeolus	Small	50	352	0.1420455
DK	feeder	Scylla	Large	50	412	0.1213592
DK	shuttle	Scylla	Large	50	435	0.1149425
DK	feeder	Scylla	Medium	50	446	0.1121076
DK	shuttle	Scylla	Medium	50	429	0.1165501
DK	feeder	Scylla	Small	47	640	0.0734375
DK	shuttle	Scylla	Small	50	442	0.1131222
DK	feeder	Windpeak	Large	50	259	0.1930502
DK	shuttle	Windpeak	Large	50	352	0.1420455
DK	feeder	Windpeak	Medium	50	367	0.1362398
DK	shuttle	Windpeak	Medium	50	369	0.1355014
DK	feeder	Windpeak	Small	50	623	0.0802568
DK	shuttle	Windpeak	Small	50	364	0.1373626

D.2 Weather experiment

Table 23: Overview of installed turbines, project duration and installation rate depending on different simulation years and alpha factors

Project	Year	Alpha	Strat	$I_{WT}^{forecast}$	Dur (d)	$I_{rate}^{forecast}$	$I_{WT}^{accuracte}$	Dur (d)	$I_{rate}^{accuracte}$
DE	2003	1	feeder	64	331	0.1934	64	298	0.2148
DE	2003	1	shuttle	56	365	0.1534	64	363	0.1763
DE	2003	1.2	feeder	43	365	0.1178	50	365	0.1370
DE	2003	1.2	shuttle	43	365	0.1178	53	365	0.1452
DE	2003	1.5	feeder	28	365	0.0767	45	365	0.1233

DE	2003	1.5	shuttle	31	365	0.0849	46	365	0.1260
DE	2015	1	feeder	52	365	0.1425	56	365	0.1534
DE	2015	1	shuttle	45	365	0.1233	50	365	0.1370
DE	2015	1.2	feeder	32	365	0.0877	37	365	0.1014
DE	2015	1.2	shuttle	35	365	0.0959	40	365	0.1096
DE	2015	1.5	feeder	28	365	0.0767	35	365	0.0959
DE	2015	1.5	shuttle	29	365	0.0795	38	365	0.1041
DE	2023	1	feeder	57	365	0.1562	61	365	0.1671
DE	2023	1	shuttle	56	365	0.1534	59	365	0.1616
DE	2023	1.2	feeder	40	365	0.1096	40	365	0.1096
DE	2023	1.2	shuttle	36	365	0.0986	41	365	0.1123
DE	2023	1.5	feeder	31	365	0.0849	38	365	0.1041
DE	2023	1.5	shuttle	38	365	0.1041	39	365	0.1068
NL	2003	1	feeder	69	203	0.3399	69	206	0.3350
NL	2003	1	shuttle	69	269	0.2565	69	268	0.2575
NL	2003	1.2	feeder	69	282	0.2447	69	288	0.2396
NL	2003	1.2	shuttle	69	316	0.2184	69	312	0.2212
NL	2003	1.5	feeder	69	287	0.2404	69	291	0.2371
NL	2003	1.5	shuttle	69	325	0.2123	69	319	0.2163
NL	2015	1	feeder	69	217	0.3180	69	223	0.3094
NL	2015	1	shuttle	69	274	0.2518	69	278	0.2482
NL	2015	1.2	feeder	69	301	0.2292	69	301	0.2292
NL	2015	1.2	shuttle	69	325	0.2123	69	340	0.2029
NL	2015	1.5	feeder	69	299	0.2308	69	299	0.2308
NL	2015	1.5	shuttle	69	324	0.2130	69	324	0.2130
NL	2023	1	feeder	69	209	0.3301	69	215	0.3209
NL	2023	1	shuttle	69	273	0.2527	69	282	0.2447
NL	2023	1.2	feeder	69	289	0.2388	69	293	0.2355
NL	2023	1.2	shuttle	69	321	0.2150	69	329	0.2097
NL	2023	1.5	feeder	69	296	0.2331	69	296	0.2331
NL	2023	1.5	shuttle	69	334	0.2066	69	320	0.2156
DK	2003	1	feeder	50	324	0.1543	50	313	0.1597
DK	2003	1	shuttle	50	287	0.1742	50	303	0.1650
DK	2003	1.2	feeder	45	365	0.1233	47	365	0.1288
DK	2003	1.2	shuttle	46	365	0.1260	50	331	0.1511
DK	2003	1.5	feeder	38	365	0.1041	47	365	0.1288
DK	2003	1.5	shuttle	36	365	0.0986	49	365	0.1342
DK	2015	1	feeder	48	365	0.1315	49	365	0.1342

DK	2015	1	shuttle	46	365	0.1260	50	298	0.1678
DK	2015	1.2	feeder	36	365	0.0986	40	365	0.1096
DK	2015	1.2	shuttle	36	365	0.0986	40	365	0.1096
DK	2015	1.5	feeder	26	365	0.0712	39	365	0.1068
DK	2015	1.5	shuttle	29	365	0.0795	37	365	0.1014
DK	2023	1	feeder	50	348	0.1437	50	334	0.1497
DK	2023	1	shuttle	50	312	0.1603	50	281	0.1779
DK	2023	1.2	feeder	39	365	0.1068	44	365	0.1205
DK	2023	1.2	shuttle	39	365	0.1068	44	365	0.1205
DK	2023	1.5	feeder	32	365	0.0877	41	365	0.1123
DK	2023	1.5	shuttle	30	365	0.0822	43	365	0.1178

D.3 Initial buffer experiment

Table 24: Overview of initial buffer experiment results for the different projects

Project	Strat	Buf	P_{time} (h)	Finish	I_{WT}	Dur (d)	I_{rate}	Cap^{feeder} (ha)	Cap^{Mars} (ha)
DE	Feeder	0	162	30-8-2023	64	516	0.124031	3.47	1.05
DE	Shuttle	0	162	26-8-2023	64	512	0.125	0.28	3.36
DE	Feeder	0	54	18-5-2023	64	412	0.15534	6.65	1.05
DE	Shuttle	0	54	13-5-2023	64	407	0.157248	0.35	7.49
DE	Feeder	0	81	29-5-2023	64	423	0.1513	6.85	1.01
DE	Shuttle	0	81	3-6-2023	64	428	0.149533	0.35	8.4
DE	Feeder	0.1	162	14-7-2023	64	469	0.136461	3.88	1.05
DE	Shuttle	0.1	162	19-7-2023	64	474	0.135021	0.28	3.71
DE	Feeder	0.1	54	13-5-2023	64	407	0.157248	6.51	1.05
DE	Shuttle	0.1	54	14-6-2023	64	439	0.145786	0.35	8.75
DE	Feeder	0.1	81	8-5-2023	64	402	0.159204	5.18	1.05
DE	Shuttle	0.1	81	20-5-2023	64	414	0.154589	0.35	6.65
DE	Feeder	0.2	162	10-6-2023	64	435	0.147126	4.2	1.05
DE	Shuttle	0.2	162	10-6-2023	64	435	0.147126	0.28	4.2
DE	Feeder	0.2	54	28-4-2023	64	392	0.163265	7.98	1.05
DE	Shuttle	0.2	54	11-5-2023	64	405	0.158025	0.35	9.45
DE	Feeder	0.2	81	14-5-2023	64	408	0.156863	5.6	1.05
DE	Shuttle	0.2	81	14-6-2023	64	439	0.145786	0.35	8.96
DE	Feeder	0.3	162	15-5-2023	64	409	0.156479	6.65	1.05
DE	Shuttle	0.3	162	20-5-2023	64	414	0.154589	0.28	6.65
DE	Feeder	0.3	54	8-5-2023	64	402	0.159204	10.03	1.05

DE	Shuttle	0.3	54	27-5-2023	64	421	0.152019	0.35	11.06
DE	Feeder	0.3	81	12-5-2023	64	406	0.157635	6.65	1.05
DE	Shuttle	0.3	81	18-5-2023	64	412	0.15534	0.35	8.4
DE	Feeder	0.4	162	18-4-2023	64	382	0.167539	8.75	1.05
DE	Shuttle	0.4	162	20-5-2023	64	414	0.154589	0.28	8.75
DE	Feeder	0.4	54	3-5-2023	64	397	0.161209	11.62	1.05
DE	Shuttle	0.4	54	26-5-2023	64	420	0.152381	0.35	13.02
DE	Feeder	0.4	81	17-4-2023	64	381	0.167979	8.75	1.05
DE	Shuttle	0.4	81	3-6-2023	64	428	0.149533	0.35	10.5
DE	Feeder	0.5	162	8-5-2023	64	402	0.159204	11.2	1.05
DE	Shuttle	0.5	162	9-5-2023	64	403	0.158809	0.28	11.2
DE	Feeder	0.5	54	19-5-2023	64	413	0.154964	13.37	1.05
DE	Shuttle	0.5	54	15-6-2023	64	440	0.145455	0.35	15.19
DE	Feeder	0.5	81	14-5-2023	64	408	0.156863	11.2	1.05
DE	Shuttle	0.5	81	9-5-2023	64	403	0.158809	0.35	11.48
DE	Feeder	0.6	162	30-4-2023	64	394	0.162437	13.3	1.05
DE	Shuttle	0.6	162	14-6-2023	64	439	0.145786	0.28	13.3
DE	Feeder	0.6	54	29-4-2023	64	393	0.16285	14.98	1.05
DE	Shuttle	0.6	54	18-6-2023	64	443	0.14447	0.35	15.82
DE	Feeder	0.6	81	8-5-2023	64	402	0.159204	13.3	1.05
DE	Shuttle	0.6	81	5-6-2023	64	430	0.148837	0.35	14.21
DE	Feeder	0.7	162	30-4-2023	64	394	0.162437	15.4	1.05
DE	Shuttle	0.7	162	5-6-2023	64	430	0.148837	0.28	15.4
DE	Feeder	0.7	54	9-5-2023	64	403	0.158809	16.38	1.05
DE	Shuttle	0.7	54	20-5-2023	64	414	0.154589	0.35	17.64
DE	Feeder	0.7	81	10-5-2023	64	404	0.158416	15.4	1.05
DE	Shuttle	0.7	81	20-5-2023	64	414	0.154589	0.35	15.68
DE	Feeder	0.8	162	10-5-2023	64	404	0.158416	17.85	1.05
DE	Shuttle	0.8	162	28-5-2023	64	422	0.151659	0.28	17.85
DE	Feeder	0.8	54	30-4-2023	64	394	0.162437	18.62	1.05
DE	Shuttle	0.8	54	18-5-2023	64	412	0.15534	0.35	19.04
DE	Feeder	0.8	81	8-5-2023	64	402	0.159204	17.85	1.05
DE	Shuttle	0.8	81	15-5-2023	64	409	0.156479	0.35	18.06
DE	Feeder	0.9	162	28-4-2023	64	392	0.163265	19.95	1.05
DE	Shuttle	0.9	162	18-5-2023	64	412	0.15534	0.28	19.95
DE	Feeder	0.9	54	14-5-2023	64	408	0.156863	20.3	1.05
DE	Shuttle	0.9	54	20-5-2023	64	414	0.154589	0.35	20.86
DE	Feeder	0.9	81	24-4-2023	64	388	0.164948	19.95	1.05

DE	Shuttle	0.9	81	27-5-2023	64	421	0.152019	0.35	20.3
DE	Feeder	1	162	28-4-2023	64	392	0.163265	22.4	1.05
DE	Shuttle	1	162	10-5-2023	64	404	0.158416	0	22.4
DE	Feeder	1	54	9-5-2023	64	403	0.158809	22.4	1.05
DE	Shuttle	1	54	21-5-2023	64	415	0.154217	0	22.4
DE	Feeder	1	81	8-5-2023	64	402	0.159204	22.4	1.05
DE	Shuttle	1	81	14-6-2023	64	439	0.145786	0	22.4
NL	Feeder	0	162	5-10-2023	69	552	0.125	0.43	0.55
NL	Shuttle	0	162	5-10-2023	69	552	0.125	0.2	0.6
NL	Feeder	0	54	1-12-2022	69	244	0.282787	1.96	0.7
NL	Shuttle	0	54	6-1-2023	69	280	0.246429	0.42	3.55
NL	Feeder	0	81	17-2-2023	69	322	0.214286	1.13	0.65
NL	Shuttle	0	81	22-2-2023	69	327	0.211009	0.3	1.45
NL	Feeder	0.1	162	21-8-2023	69	507	0.136095	1.5	0.67
NL	Shuttle	0.1	162	18-8-2023	69	504	0.136905	0.2	1.5
NL	Feeder	0.1	54	12-11-2022	69	225	0.306667	1.85	0.7
NL	Shuttle	0.1	54	20-12-2022	69	263	0.262357	0.42	3.75
NL	Feeder	0.1	81	21-1-2023	69	295	0.233898	1.5	0.6
NL	Shuttle	0.1	81	30-1-2023	69	304	0.226974	0.3	1.6
NL	Feeder	0.2	162	25-6-2023	69	450	0.153333	3.25	0.55
NL	Shuttle	0.2	162	27-6-2023	69	452	0.152655	0.2	3.25
NL	Feeder	0.2	54	21-10-2022	69	203	0.339901	3.25	0.6
NL	Shuttle	0.2	54	19-12-2022	69	262	0.263359	0.42	5.18
NL	Feeder	0.2	81	18-12-2022	69	261	0.264368	3.25	0.7
NL	Shuttle	0.2	81	22-12-2022	69	265	0.260377	0.3	3.25
NL	Feeder	0.3	162	29-4-2023	69	393	0.175573	5	0.6
NL	Shuttle	0.3	162	30-4-2023	69	394	0.175127	0.2	5
NL	Feeder	0.3	54	20-10-2022	69	202	0.341584	5	0.75
NL	Shuttle	0.3	54	19-12-2022	69	262	0.263359	0.42	6.75
NL	Feeder	0.3	81	16-11-2022	69	229	0.30131	5	0.7
NL	Shuttle	0.3	81	19-12-2022	69	262	0.263359	0.3	5
NL	Feeder	0.4	162	9-3-2023	69	342	0.201754	6.75	0.75
NL	Shuttle	0.4	162	9-3-2023	69	342	0.201754	0.2	6.75
NL	Feeder	0.4	54	21-10-2022	69	203	0.339901	6.75	0.75
NL	Shuttle	0.4	54	19-12-2022	69	262	0.263359	0.42	8
NL	Feeder	0.4	81	22-10-2022	69	204	0.338235	6.75	0.75
NL	Shuttle	0.4	81	22-12-2022	69	265	0.260377	0.3	6.75
NL	Feeder	0.5	162	17-1-2023	69	291	0.237113	8.5	0.75

NL	Shuttle	0.5	162	17-1-2023	69	291	0.237113	0.2	8.5
NL	Feeder	0.5	54	20-10-2022	69	202	0.341584	8.5	0.75
NL	Shuttle	0.5	54	22-12-2022	69	265	0.260377	0.42	9.5
NL	Feeder	0.5	81	20-10-2022	69	202	0.341584	8.5	0.75
NL	Shuttle	0.5	81	19-12-2022	69	262	0.263359	0.3	8.5
NL	Feeder	0.6	162	18-11-2022	69	231	0.298701	10.25	0.75
NL	Shuttle	0.6	162	22-12-2022	69	265	0.260377	0.2	10.25
NL	Feeder	0.6	54	20-10-2022	69	202	0.341584	10.25	0.75
NL	Shuttle	0.6	54	26-12-2022	69	269	0.256506	0.42	11.25
NL	Feeder	0.6	81	20-10-2022	69	202	0.341584	10.25	0.75
NL	Shuttle	0.6	81	21-12-2022	69	264	0.261364	0.3	10.25
NL	Feeder	0.7	162	21-10-2022	69	203	0.339901	12	0.75
NL	Shuttle	0.7	162	20-12-2022	69	263	0.262357	0.2	12
NL	Feeder	0.7	54	20-10-2022	69	202	0.341584	12	0.6
NL	Shuttle	0.7	54	19-12-2022	69	262	0.263359	0.42	12.4
NL	Feeder	0.7	81	20-10-2022	69	202	0.341584	12	0.75
NL	Shuttle	0.7	81	21-12-2022	69	264	0.261364	0.3	12
NL	Feeder	0.8	162	20-10-2022	69	202	0.341584	13.75	0.75
NL	Shuttle	0.8	162	19-12-2022	69	262	0.263359	0.2	13.75
NL	Feeder	0.8	54	20-10-2022	69	202	0.341584	13.75	0.6
NL	Shuttle	0.8	54	22-12-2022	69	265	0.260377	0.42	14
NL	Feeder	0.8	81	20-10-2022	69	202	0.341584	13.75	0.75
NL	Shuttle	0.8	81	22-12-2022	69	265	0.260377	0.3	13.75
NL	Feeder	0.9	162	21-10-2022	69	203	0.339901	15.5	0.75
NL	Shuttle	0.9	162	22-12-2022	69	265	0.260377	0.2	15.5
NL	Feeder	0.9	54	20-10-2022	69	202	0.341584	15.5	0.75
NL	Shuttle	0.9	54	21-12-2022	69	264	0.261364	0.35	15.5
NL	Feeder	0.9	81	20-10-2022	69	202	0.341584	15.5	0.75
NL	Shuttle	0.9	81	21-12-2022	69	264	0.261364	0.25	15.5
NL	Feeder	1	162	20-10-2022	69	202	0.341584	17.25	0.75
NL	Shuttle	1	162	23-12-2022	69	266	0.259398	0	17.25
NL	Feeder	1	54	21-10-2022	69	203	0.339901	17.25	0.75
NL	Shuttle	1	54	24-12-2022	69	267	0.258427	0	17.25
NL	Feeder	1	81	20-10-2022	69	202	0.341584	17.25	0.75
NL	Shuttle	1	81	21-12-2022	69	264	0.261364	0	17.25
DK	Feeder	0	162	28-5-2023	50	422	0.118483	3.25	2.4
DK	Shuttle	0	162	6-6-2023	50	431	0.116009	0.55	4.45
DK	Feeder	0	54	6-4-2023	50	370	0.135135	10	2.5

DK	Shuttle	0	54	30-3-2023	50	363	0.137741	4.4	7.95
DK	Feeder	0	81	3-4-2023	50	367	0.13624	7.95	2.05
DK	Shuttle	0	81	14-4-2023	50	378	0.132275	2.3	7.55
DK	Feeder	0.1	162	17-4-2023	50	381	0.131234	2.7	1.6
DK	Shuttle	0.1	162	29-4-2023	50	393	0.127226	0.55	4.15
DK	Feeder	0.1	54	21-3-2023	50	354	0.141243	10.9	2.4
DK	Shuttle	0.1	54	8-3-2023	50	341	0.146628	3.9	7.4
DK	Feeder	0.1	81	30-3-2023	50	363	0.137741	7.4	2.1
DK	Shuttle	0.1	81	9-4-2023	50	373	0.134048	2.2	6.3
DK	Feeder	0.2	162	3-4-2023	50	367	0.13624	5	2.05
DK	Shuttle	0.2	162	30-3-2023	50	363	0.137741	0.55	5
DK	Feeder	0.2	54	3-4-2023	50	367	0.13624	12.4	2.35
DK	Shuttle	0.2	54	19-3-2023	50	352	0.142045	3.5	9.85
DK	Feeder	0.2	81	19-3-2023	50	352	0.142045	8.9	2.05
DK	Shuttle	0.2	81	1-3-2023	50	334	0.149701	2.05	7.25
DK	Feeder	0.3	162	20-3-2023	50	353	0.141643	7.5	2.2
DK	Shuttle	0.3	162	1-3-2023	50	334	0.149701	0.55	7.5
DK	Feeder	0.3	54	20-3-2023	50	353	0.141643	13.9	2.35
DK	Shuttle	0.3	54	10-3-2023	50	343	0.145773	3.4	11.6
DK	Feeder	0.3	81	31-3-2023	50	364	0.137363	11.3	2.5
DK	Shuttle	0.3	81	30-3-2023	50	363	0.137741	1.85	9.05
DK	Feeder	0.4	162	3-4-2023	50	367	0.13624	10	2.5
DK	Shuttle	0.4	162	30-3-2023	50	363	0.137741	0.55	10
DK	Feeder	0.4	54	3-4-2023	50	367	0.13624	15.2	2.05
DK	Shuttle	0.4	54	20-3-2023	50	353	0.141643	2.7	13.35
DK	Feeder	0.4	81	8-4-2023	50	372	0.134409	13	2.05
DK	Shuttle	0.4	81	30-3-2023	50	363	0.137741	1.7	11.45
DK	Feeder	0.5	162	19-3-2023	50	352	0.142045	12.5	2.1
DK	Shuttle	0.5	162	1-3-2023	50	334	0.149701	0.45	12.5
DK	Feeder	0.5	54	21-3-2023	50	354	0.141243	16.6	2.05
DK	Shuttle	0.5	54	30-3-2023	50	363	0.137741	2.6	14.2
DK	Feeder	0.5	81	19-3-2023	50	352	0.142045	14.4	2.05
DK	Shuttle	0.5	81	10-4-2023	50	374	0.13369	1.4	13.9
DK	Feeder	0.6	162	21-3-2023	50	354	0.141243	15	2.05
DK	Shuttle	0.6	162	30-3-2023	50	363	0.137741	0.45	15
DK	Feeder	0.6	54	3-4-2023	50	367	0.13624	18.1	2.5
DK	Shuttle	0.6	54	19-3-2023	50	352	0.142045	2.2	16.75
DK	Feeder	0.6	81	21-3-2023	50	354	0.141243	17	2.05

DK	Shuttle	0.6	81	10-3-2023	50	343	0.145773	1.2	15
DK	Feeder	0.7	162	8-4-2023	50	372	0.134409	17.5	2.5
DK	Shuttle	0.7	162	31-3-2023	50	364	0.137363	0.45	17.5
DK	Feeder	0.7	54	4-4-2023	50	368	0.13587	19.8	2.5
DK	Shuttle	0.7	54	3-4-2023	50	367	0.13624	1.8	18.45
DK	Feeder	0.7	81	30-3-2023	50	363	0.137741	18.4	2.5
DK	Shuttle	0.7	81	20-3-2023	50	353	0.141643	1.05	17.5
DK	Feeder	0.8	162	20-3-2023	50	353	0.141643	20	2.05
DK	Shuttle	0.8	162	31-3-2023	50	364	0.137363	0.45	20
DK	Feeder	0.8	54	3-4-2023	50	367	0.13624	21.5	2.5
DK	Shuttle	0.8	54	20-3-2023	50	353	0.141643	1.2	20.25
DK	Feeder	0.8	81	21-3-2023	50	354	0.141243	20.3	2.35
DK	Shuttle	0.8	81	3-4-2023	50	367	0.13624	0.85	20
DK	Feeder	0.9	162	20-3-2023	50	353	0.141643	22.5	2.2
DK	Shuttle	0.9	162	3-4-2023	50	367	0.13624	0.45	22.5
DK	Feeder	0.9	54	18-3-2023	50	351	0.14245	23.2	2.05
DK	Shuttle	0.9	54	19-3-2023	50	352	0.142045	0.8	22.5
DK	Feeder	0.9	81	20-3-2023	50	353	0.141643	22.8	2.05
DK	Shuttle	0.9	81	21-3-2023	50	354	0.141243	0.65	22.5
DK	Feeder	1	162	30-3-2023	50	363	0.137741	25	2.05
DK	Shuttle	1	162	10-3-2023	50	343	0.145773	0	25
DK	Feeder	1	54	21-3-2023	50	354	0.141243	25	2.05
DK	Shuttle	1	54	5-4-2023	50	369	0.135501	0	25
DK	Feeder	1	81	3-4-2023	50	367	0.13624	25	2.35
DK	Shuttle	1	81	30-3-2023	50	363	0.137741	0	25